TRIBHUVAN UNIVERSITY

INSTITUTE OF ENGINEERING

PULCHOWK CAMPUS

STRUCTURAL SUITABILITY OF MASONRY STRUCTURE FOR RESIDENTIAL BUILDINGS IN RURAL AREAS OF NEPAL

BY

KAMAL PAUDEL

A THESIS REPORT

SUBMITTED TO THE DEPARTMENT OF CIVIL ENGINEERING

IN PARTIAL FULFILLMENT OF THE REQUIREMENTS FOR THE

DEGREE OF MASTER IN

STRUCTURAL ENGINEERING

DEPARTMENT OF CIVIL ENGINEERING

LALITPUR, NEPAL

SEP, 2021

COPYRIGHT

……………………………….

Head of Department

Department of Civil Engineering

Institute of Engineering

Pulchowk Campus

Lalitpur, Nepal

TRIBHUVAN UNIVERSITY

INSTITUTE OF ENGINEERING

PULCHOWK CAMPUS

DEPARTMENT OF CIVIL ENGINEERING

The undersigned certify that they have read, and recommended to the Institute of Engineering for acceptance, a thesis entitled "**Structural Suitability of Masonry Structure for Residential Buildings in Rural Areas of Nepal**" submitted by Kamal Paudel (075/MSStE/005) in partial fulfilment of the requirements for the degree of Master of Science in Structural Engineering.

____

Supervisor, Prof. Dr. Hari Darsan Shrestha
Department of Civil Engineering
M.Sc. Structural Engineering
Pulchowk Campus, Lalitpur, Nepal

____

External Examiner, Dr Suman Narsingh Rajbhandari

____

Program Coordinator, Prof. Dr. Kamal Bahadur Thapa
Department of Civil Engineering
M.Sc. Structural Engineering
Pulchowk Campus, Lalitpur, Nepal

ABSTRACT

Construction of masonry structures using different kinds of masonry units is still widely in practice in the rural area and suburban part of Nepal. For the suitability of the building and its implementation evaluation of seismic performance is required. Its affordability and use of local material in construction also govern the suitability of structures in a different locations.

For this four typologies of the building based on reconstruction in 32 districts after the Gorkha earthquake was considered for the analysis. These four buildings are of different mechanical properties and wall thickness but all of them have common usable space. These buildings were modelled using finite element software and analysis by using linear dynamic analysis. In this study, the damage is idealized as the maximum top storey displacement of each building. Three-time histories (Gorkha, Imp Valley and Kobe) were used for the linear dynamic analysis. Base shear, displacement and drift of different buildings using different PGA of an earthquake were determined. By using the First-order second moment method probability of failure of each building were determined and a fragility curve was generated.

These fragility curves were compared to understand the seismic performance characteristic of the selected structural system. Material and labor required for the building were estimated using standard norms of Nepal. The total cost of the selected building system was calculated using rate of Rammechhap district. The result shows that the Lateral displacement and storey drifts are considerably reduced while the contribution of brick wall with cement mortar (BCEM) is taken into account. The probability of failure of a different building is a smaller percentage in the analysis of houses applying the Gorkha Earthquake than the other two earthquakes (Imp Valley and Kobe) earthquake. Also, the cost of SMUD typology is found to be lowest and use of local material in SMUD typology is highest among four typologies.

ACKNOWLEDGEMENT

I would like to express my deep gratitude to my thesis supervisor, Professor Dr. Hari Darshan Shrestha, for his valuable guidance, strong motivation, continuous encouragement and support throughout the whole thesis work. His technical excellence, motivational ideas and suggestions have helped me in the critical stages of the thesis.

I am also grateful to all my teachers, and seniors specially Er. Shyam Sundar Basukala and Er. Kshitiz Paudel, for their valuable suggestions and good cooperation during thesis work.

Similarly, I would like to express my sincere thanks to my classmates, for their direct and indirect cooperation, advice and help during the period of master's study as well as in this thesis.

Lastly, I am very thankful to my family for their continuous support, constant encouragement and patience at every moment of thesis work.

Kamal Paudel

075/MSStE/005

TABLE OF CONTENTS

LIST OF TABLES

LIST OF FIGURES

LIST OF SYMBOLS AND ABBREVIATIONS

ADRS	Acceleration displacement response spectrum
BCEM	Brick masonry with cement mortar
βd βc	Standard deviation of demand, standard deviation of capacity
β_{SPGA}	The square- root-sum-of-the-squares combination of individual variability
C	Capacity of the structure
CBS	Central Bureau of statistics
CFP	Common Feedback Project
CGI	Corrugated Galvanized iron
C.o.V	Coefficient of Variation
CSEB	Compressed Stabilized Earth Block
d_u	ultimate displacement
DUDBC	Department of Urban Development and Building Construction
d_y	yield displacement
D	Demand of the structure DPM Damage probability matrices
E	Modulus of elasticity
f_{ck}	Characteristics strength of concrete
f_y	Specified minimum yield strength
G	Shear Modulus
FEMA	Federal Emergency Management Agency
FOSM	First Order Second Moment method
HRRP	Housing Recovery and Reconstruction Platform
PEH	Potential Earthquake Hazards
PGA	Peak ground Acceleration
PGD	Peak ground Displacement
PGV	Peak ground velocity
p_f	Probability of failure PGA Peak Ground Acceleration
PS	Performance Score
PSDM	Probabilistic seismic demand m
R	Response of the structure
SAP	Structural Analysis Program
SVA	Seismic Vulnerability Assessment

S_d	Mean value of demand SDOF Single degree- of-freedom
S_c	Mean value of capacity
SCEM	Stone masonry with Cement mortar
SMUD	Stone masonry with Mud mortar
UTM	Universal testing machine

1 INTRODUCTION

1.1 Background

Earthquake is one of the most natural disastrous phenomena, which can happen at any time without any warnings and can destroy building structures, killing or injuring the inhabitants, and is, therefore, unpredictable and unpreventable. The earthquakes may occur as a result of tectonic activity, volcanic activity, landslides and rock falls, and nuclear explosions. In the context of Nepal, the most probable natural disaster phenomenon is the earthquakes that are caused by tectonic activity. Nepal is situated along the southern slope of the Himalayan Mountain range, which is susceptible to frequent earthquakes of different magnitudes. About 75% of fatalities attributed to the earthquake are caused by the collapse of buildings. This is probably due to the lack of proper use of material and technology to rationally consider the effect of lateral forces due to possible earthquakes. Recently built large public buildings are designed and detailed according to the prevalent seismic codes and construction works are carried out with relatively better-quality control. However, in rural areas of Nepal, most of the small and residential buildings are built without proper design and with little or no engineering input.

Masonry has been used in a wide variety as a basic construction material for the public as well as residential buildings in rural and periphery of an urban area of Nepal. Masonry is the most important construction material used for different construction purpose. It has been used from past several thousands of years to present. A great number of national heritage structures had been made of masonry and some of them have survived in past earthquakes also. In most of the rural areas of Nepal, the construction of RCC framed structure building is not possible due to many constraints like the fund, availability of materials and availability of skilled workmanship. Therefore, the construction of masonry buildings is only the means of housing in rural areas of our country.

The government and private sectors are investing a massive amount of resources and funds in building construction. The vision of the 15th periodic plan is to provide safe, affordable and environmentally-friendly buildings. Therefore, it has become necessary to make a study and research on the construction material and technology available in the country; to make optimum use of local materials; to enhance the use of economical, simple, easily available, and appropriate material having no adverse effects on the environment. Research should be focus towards to make improvements in the construction of rural housing in a planned way, gaining necessary services in rural housing, and maintaining a balance between the income of rural residents and their minimum housing construction cost.

The materials should be made of local and low cost components. The high cost of the construction process for rural building construction is a major problem for those people who want to have access to this basic need in developing countries like Nepal. One alternative solution to this situation is the proper use of locally available material and the discovery of new suitable building materials expected to reducing construction costs. The use of these local building materials can effectively reduce construction costs both for labor and materials at the same time as improving the thermal comfort conditions in domestic buildings. These alternative techniques can also be applied to promote beneficial multiple effects in the rural area of Nepal, and if they are applied at massive levels. They can contribute to reducing the high housing deficit in our country.

The current construction practices in Nepal (i.e. framed structure) are often unaffordable for the low-income public in rural areas. If these construction of buildings and services are too expensive, the low income people of these different areas cannot afford to live there. Job creating activities such as labor-intensive construction methods may perhaps present another way of obtaining local economical sustainability. The use of sustainable sound building materials has to be incorporated throughout the country. Appropriate technology is very important when discussing the suitability of structure. The use of technology has to be following the local conditions and at the same time be durable, reliable, and functionally constructed to a modern life.

Most of the masonry structures in the rural area of Nepal were constructed from the combination of masonry walls, wooden floor, and tile/CGI sheet roof system. The integrity between the different elements of the structures has not been considered well. Particularly, the main component of such structures is load-bearing masonry walls. Generally, the load-bearing masonry is made of stone bricks and block with cement or mud mortar. Therefore, such structures are most vulnerable during an earthquake. As a result, certain building factors should be considered during the design and construction of masonry structures.

Modern structural engineers have limited knowledge of old materials and procedures as concrete and steel have become the primary building materials in most of Nepal's urban and suburban districts. The lack of information about old materials and processes creates a strong bias in the rehabilitation of existing structures and prevents accurate safety assessments. It is important not only to preserve old structures but also to construct and preserve them using the traditional methods of construction with suitable material. This research focused on different types of building typologies and material that can be constructed with maximum use of local material.

1.2 Need of Research

People have now become very conscious about the safety of the building against earthquake forces with the increase in awareness of seismic vulnerability. Though the modernization of building technology has resulted in reinforced concrete structures. Construction of masonry structures using different kinds of masonry units is still widely in practice in the rural area and suburban part of Nepal. For the suitability of the building and its implementation evaluation of seismic performance is required. The seismic performance is related to the strength and damage level of the structure that is expected to undergo during the earthquake. Study of fragility analysis is therefore required to give the probability of damage to a given building type due to earthquake.

Building regulations are mandatory standards for the design and construction of buildings to ensure the safety and health of people. While constructing a building the economic aspect mostly governs the type of construction technique to be used. Though the people have their own preferences, low-cost housing ultimately seems more lucrative. Due to the large variation of topological and geological environment in our country the building materials vary from place to place. But the selection of these materials and the technology to be adopted during construction should be kept in mind. Besides this, the availability of skill workmanship is also governing factor to choose a building technology type.

In the last two decades, many new access roads have been constructed, but most of these roads are operable in dry weather only. These conditions of roads in the rural area of Nepal limits access to markets for purchasing cement, bricks, rebar, and iron sheets and creates logistical challenges for transporting these building materials, even if funds are available, as these construction materials have to be carried manually from market to construction sites. Thus, the main purpose of this study is to identify the different local materials that are suitable in terms of seismic performance and cost that can be affordable by a low-income group of the country.

1.3 Research Objectives

- To determine seismic performance of masonry structure excited by different ground motion time histories.
- To recommend the suitable structure for rural area in terms of seismic performance, cost and use of local material.

1.4 Methodology

As the basic aim of this research work is to evaluate the seismic performance of masonry buildings and to find the suitability of masonry structure, the methodology adopted for these works are elaborated with the various works:

1. Review of various literature concerning different typologies of building, characteristics of masonry structures, types of materials, modelling strategy for the masonry building, and analysis technique for masonry building.
2. Four types of typical buildings have been proposed. These buildings will be suitable for rural areas having family (4-6) members.

    Brick masonry with Cement mortar (BCEM)
    Stone masonry with Cement mortar (SCEM)
    Stone masonry with mud mortar (SMUD)
    Cement mortar CSEB blocks (CSEB)

All available data of material required for a building has been obtained from past research and documents.

3. Preparation of simulation model of each type of building in SAP 2000, and determine the response of buildings in terms of displacement at different scale of PGA by Time History analysis.
4. Generation of Fragility Curve at four damage states specified by (HAZUS 4.2 SP3 2020) for each type of buildings. This will enable us to know the seismic performance of the proposed building during different PGA earthquakes.
5. Results obtained from the analysis are compared to understand the performance characteristic of the selected structural system.

6. Different materials were estimated for every type of building. Labor required for the work was determined from the standard norms for civil work of Nepal for different work.
7. Ramechhap district was selected for cost calculation. The construction costs are computed for different structural and nonstructural elements and a comparison of each typology was performed.
8. Determination of suitability of masonry structure based on seismic performance, cost, and use of local materials.

1.5 Scope and Limitation of Study

The scope of this study is to investigate the behaviour of masonry buildings constructed from Brick, stone, and CSEB blocks and to find the economic benefit of different materials used in building structures. These buildings have a different level of vulnerability by the virtue of their difference in material properties, and wall thickness. For this purpose, detailed structural analyses of the building have been classified into four types based on their material properties. This research work is based on these four typologies of buildings with timber floor diaphragms.

In this research linear time history analysis of masonry structure has been carried out using different earthquakes to determine demand displacement. In opposition to the typical RC framed concrete structures, where it is easy to identify the yield hinges, nonlinear time history analysis of masonry structures is complex and takes a long time for the model considered.

For the capacity of the building, the guidelines of (HAZUS 4.2 SP3 2020) has been followed. Pushover analysis for the capacity of masonry buildings could have been done but due to insufficient data for nonlinear static analysis pushover analysis was not done which is the limitation of this thesis. The finite element study of the masonry buildings is carried out using homogeneous elements in SAP 2000v22. The effect of nonlinearity is not considered in dynamic analysis. Temperature, Creep, and fatigue effects are not considered in the analysis of structure which is another limitation of this research.

1.6 Organization of thesis

The works has been presented in five chapters.

Chapter l includes Introduction to the research, Needs and Objectives of the study along with Methodology, Scope and Limitations of the study are also presented in this chapter.

Chapter 2 includes relevant literature reviews. The literatures reviewed are mainly related with building typologies, material properties, failure mechanism, modelling techniques for masonry structure and analysis of masonry structures.

Chapter 3 outlines the modeling and analysis part of the masonry structures. The considered configuration, material properties and different analysis tools are presented. The detail about macro element modelling of masonry structure are also presented in this chapter. This chapter describes in detail about time history analysis and generation of fragility curves using First Order Second Moment (FOSM) method.

Chapter 4 presents the results and discussion of the research. The result includes response in terms of displacement and base shear. The fragility curves of four types of buildings considering three types of earthquake ground motion time histories were plotted and described in this chapter. This chapter also includes result of different material and cost for each typologies.

Chapter 5 presents major conclusion of the thesis work and recommendations for further study.

2 LITERATURE REVIEW

2.1 General

Masonry buildings in Nepal exhibited severe destruction and collapse in recent strong earthquake events like Gorkha earthquake 2015. It is known that their brittle behavior of the masonry structure which is mainly due to the combination of different case like low tensile strength, large mass and improper connection between the different structural elements. Most of the research in Nepal are concentrated to find out the seismic performance of existing masonry structure but limited research are available to find the seismic performance of new typologies of masonry that are suitable for future. 'Scientific authentication of seismic behavior is needed before propagating the concept of masonry structures'(Dixit et al., 2004).

Gautam et al. (2016) describe the frequent collapse types in Nepalese structures following the MW 7.8 Gorkha (Nepal) earthquake.During the reconnaissance assessment conducted immediately after the earthquake on April 25, 2015, several sorts of damage patterns were found for reinforced concrete buildings as well as masonry houses. They found that the major cause of failure in masonry structures are construction and structural deficiencies. They found that the implementation of building codes and improvement mechanisms are largely lagging in most of the rural areas of Nepal. Horizontal bands are seldom noticed in masonry structures and found that masonry structures with bands were less damaged than structures without bands. They suggest that for the rural area of Nepal, earthquake-resistant technology should be propagated and older structures should be replaced by locally available material with suitable new technology.

Dixit et al. (2004) surveyed vernacular building types in various parts of Nepal. The study revealed several earthquake-resistant features being incorporated in local building constructions. The survey results conclude that traditionally made masonry structures are stronger than expected and they will not generate pancake destruction like RC framed structures. 40% of the masonry building in Nepal remained unaffected seriously in the 1934 earthquake.

This research suggests that Study, exploration and analysis are necessary not only because people living in such masonry construction and therefore continue building such construction in foreseeable future but also Several of the building typologies that are constructed by people are not fully understood and described. So, it is necessary to make a statement of seismic stability of such typologies of buildings. This research suggests that Scientific authentication of seismic behaviour is needed before propagating or revitalizing the traditional concepts of the masonry structure. Also, it suggests that affordability, acceptability, and ease in implementation as well as in communicating the knowledge should perhaps be some of the criteria for selecting the concepts for scientific researches.

Ali et al. (2014) studied the seismic behaviour of stone masonry structures. Different models in this research are representative school building, a residential building, and a model that include simple cost-effective features in the form of horizontal and vertical reinforced concrete elements. The findings of this study reveal that adopting cost-effective elements such vertical members in joints and corners, as well as relatively thin horizontal bands, can greatly improve the seismic performance of stone masonry in various masonry structures.

Karasin et al. (2017) studied the structural damage after the Gorkha earthquake. The research observed that the negative features of constructions in structure have caused an increase in damage level. This research found that most of the damaged buildings have not been constructed according to NBC codes and suggest that necessary research have to be done to know about building properties and to know the seismic behaviour of the structure under earthquake.

Gautam (2018) studied the seismic vulnerability of different rural stone masonry buildings affected by the 2015 Gorkha earthquake. The result in this research shows that many of the masonry building in rural area in Nepal would observed severe damage or collapse in the case of strong to major earthquakes. The results shows that there is need of new advancement of technology to reduce the damage and vulnerability of building to prevent the loss of property and life of human. The research suggests that further analysis is required to construct fragility function.

Gautam and Chaulagain (2016) studied the structural performance and associated lessons to be learned from world earthquakes in Nepal after Gorkha earthquake. They found that structural vulnerability of masonry structures in rural areas is very high due to age, construction materials, separated walls, poor binding of material, heavy roofing material like stone, poor connection between junction of walls walls, and diaphragm discontinuity among others. They found that during Gorkha earthquake mainly structural damage is due to the lack of quality of material, high age of building, deficient construction practices, poor binding materials, local site effects etc. They suggest that so selection of proper strengthening solution and justification should be assured before implementation. Also, they suggest that Strengthening should be based on detailed field assessment of building and scientific structural analysis rather than imposing whatever is available with the contactors and client.

2.2 Literature related to Building Typology

HRRP (2018) provides examples of the wide range of housing types being constructed across the 32 districts affected by the April 2015 Gorkha earthquake. Graph 2-1 below presents a comparison of the prevalence of typologies pre and post-earthquake. The pre-earthquake data is from the Central Bureau of Statistics (CBS) damage assessment. The post-earthquake data is from an analysis carried out by HRRP and the Inter-Agency Common Feedback Project (CFP) in May 2018.

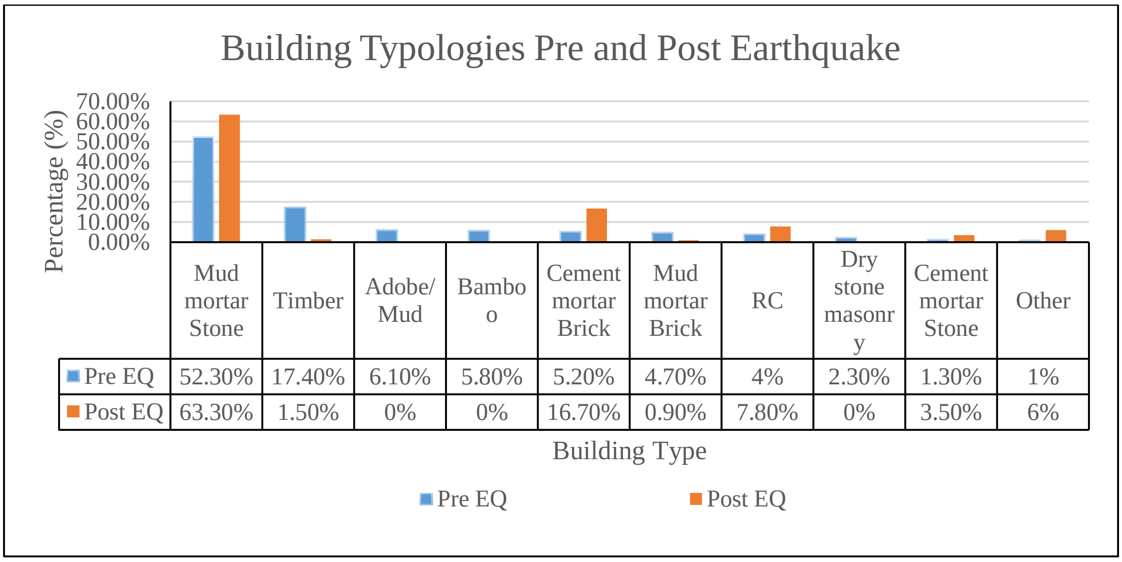

Figure 2-1: Graph showing Building Typologies Pre and post-Earthquake

The typology considered in this research is based on the basic reconstruction program in earthquake-affected areas so that it could represent a true scenario of Nepal.

Number of members in household (CBS 2012)

National Population and Housing Census 2011 (CBS 2012) shows that 840,205 households in rural areas have 4 members, 800,608 households have 5 members and 632,170 households in rural areas have 6 members. These data show that more than

50% of households in rural areas have 4-6 members. The size of the building considered in this research is based on the number of members in the household that is suitable for 4-6 members.

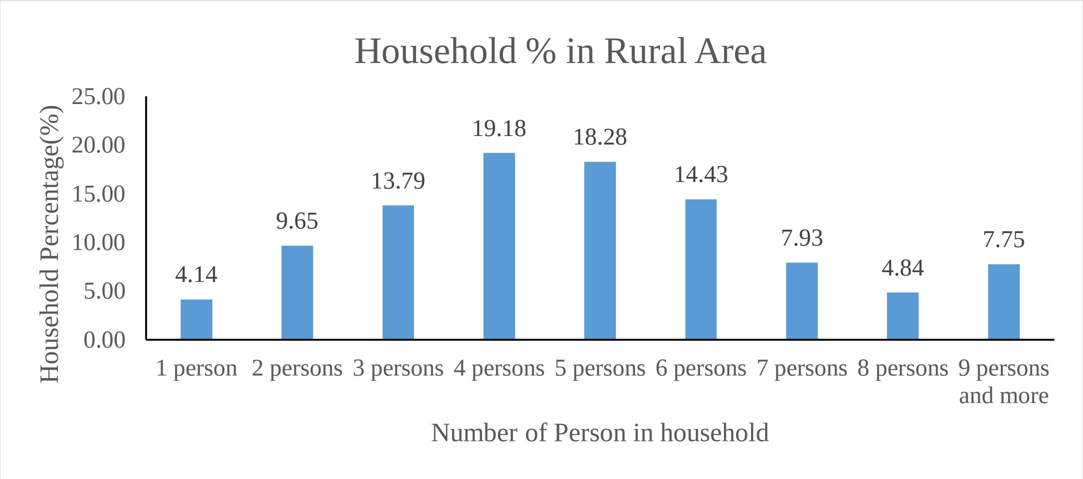

Figure 2-2: Household % in rural area

Selection of building plan and elevation

For the selection of the building plan reconstruction report from HRRP, past literature, design manual, and available pictures have been studied. Most of the rural area of Nepal lies in slope ground. So, it is difficult to get flat land in most of the rural areas and rare to find the same length and breadth. It is found that most buildings have a length to breadth ratio. The length of the building was found to be 2-3 times greater than breadth. The plan considered in this study is based on a length to breadth ratio of about 2 so that they may be useful for future practice and construction for different rural areas of Nepal. Room size Considered in this research is based on the average size of the room suggested by DUDBC Volume I and Volume II.

a b

Figure 2-3: Dense row settlement in western Nepal a. (Arghakhanchi, Chhatradev Rural Municipality Ward No. 01) b. (Lamjung, kwholasothar rural Municipality Ghale Gaun) (Source: Naresh Paudel and Prakriti Sharma)

a b

Figure 2-4: Building constructed after Gorkha Earthquake a. ((Kavrepalanchok, ChauriDeurali Rural Municipality, Ward No. 5), Gimdi) b. (Sindhuli, Sunkoshi Rural Municipality, Ward No 5) (Source: HRRP 2018)

a b

Figure 2-5: Building constructed after Gorkha Earthquake a. (Lalitpur, Bagmati Rural Municipality, Ward No. 4, Gimdi) b. Earthquake (Ramechhap, Ramechhap Municipality, Ward No. 9) (Source: HRRP 2018)

2.3 Literature related to material properties

Phaiju and Pradhan (2018) studied the different mechanical properties of brick and masonry panels. The study has been concentrated on finding the compressive strength and Young's modulus of elasticity of brick, mortar, and masonry. The study was done experimentally for the brick samples that are generally used in Nepal. The structural testing laboratory of Khwopa Engineering College which has a Universal Testing Machine (UTM) of 40 Tonne capacity was used for loading purposes. The material used in this experiment was first-class brick, 4.75mm passed sand, and OPC 53 grade cement. The Young's modulus of masonry panel observed from the experiment suggests that the value was 2703.2N/mm2 and the compression strength of the Masonry Panel was 2.5 N/mm2. The shear test result showed that the modulus of rigidity of the brick panel was found to be 915.1 N/mm2. From the experimental work, Poisson's ratio for masonry panels is found to be 0.32.

Magenes et al. (2010) conducted an experimental program that includes shake-table tests on three full-scale prototype buildings, a set of tests on single walls has been performed for the characterization of mechanical properties of stone masonry with cement sand mortar. These tests include diagonal compression, vertical compression, and in-plane cyclic shear tests. Elastic properties of masonry (Young and shear moduli, Poisson ratio) have been derived from vertical and diagonal compression tests. The Young's modulus of masonry panel observed from the experiment suggests that the value was 2550N/mm^2 and the compression strength of the Masonry Panel was 3.28N/mm^2 with C.o.V 8 %. The tensile strength of stone masonry from this experiment was 0.137N/mm2. The shear test result showed that the modulus of rigidity of the brick panel was found to be 840 N/mm2. From the experimental work, Poisson's ratio for masonry panels is found to be 0.25.

Meimaroglou and Mouzakis (2018) presented the experimental investigation of the mechanical properties of masonry constructed with natural stones and clay (mud) mortars under compression focusing on the production and properties of the mortars. Soil for the masonry was collected and prepared (crushing of clods, sieving, drying, and mixing). Raw materials used for the production of the mortars were evaluated by examining the particle size distribution by hydrometer and by sieves and by measuring the concentration of the total soluble salts and the organic material. After a six-month maturation period, the brick wall was subjected to monotonic compression to determine the compressive strength and modulus of elasticity. They found that the average compressive strength of masonry was 4 MPa, which is comparable to the compressive strength of the mortar. The obtained strength in this research can be considered high compared to values reported by other researchers varying between 1 and 3.7 MPa. The experimental results from the compression tests on the wallets show that Young's modulus of elasticity of the wall is 502.19 N/mm^2. Poisson’s ratio for masonry panel is found to be 0.20.

Mellegard and Steinert (2016) studied the compressed stabilized earth block in the rural village of Nepal (Majhi Gaun after the Gorkha earthquake. The purpose of this study is to make a structural analysis of a CSEB building, to investigate the real material properties of the CSEB block, and to study the structural behaviour of a CSEB building in Nepal. The goal of this research was to determine values for the parameters Young's modulus, density, compressive and tensile strength, and the first natural period of a CSEB structure. Young's modulus of elasticity of CSEB block was found to be 851 N/mm2, which is almost the same as that value suggested by (Shrestha, Standard Norms and Specification for CSEB Block, 2012). Poisson ratio for CSEB block suggested in this research was 0.25. The density ranged from 1470.6-1719.5 kg/m3 with an average of 1548kg/m3. The mean values for the tensile and compressive strength of the CSEB were 1.78 MPa and 11.1 MPa which is more than the value suggested by (Shrestha, 2012).

2.4 Literature related to Failure modes

Different characteristics such as the quality of materials, the geometry, the load application, and boundary conditions influence the type of failure mode of masonry walls under in-plane seismic loads. From experimental results as well as analysis of earthquake damages, three types of failure modes have been identified. They are sliding shear, diagonal shear and flexural failure. These failure modes are illustrated in Figure 2-6.

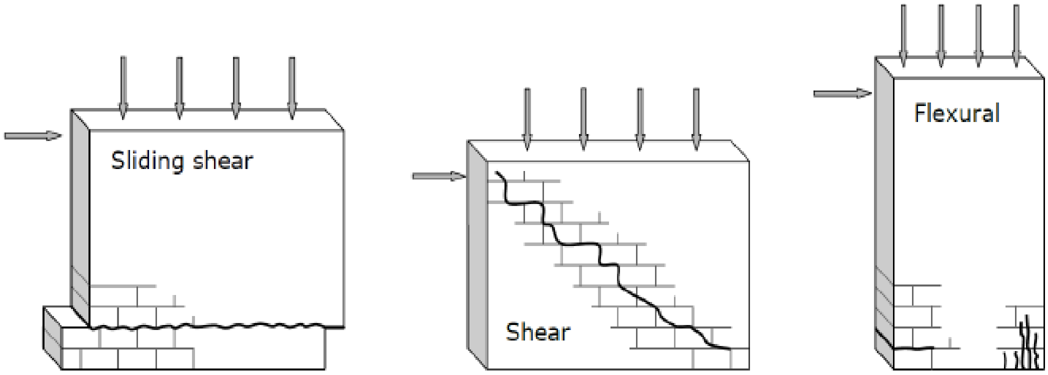

Figure 2-6: Failure Modes of Masonry Walls (Tomazevic, 1999)

Sliding shear failure occurs due to the use of poor-quality mortar and low vertical load acting on the wall. Loads induced by seismic actions shear the wall in two parts along horizontal mortar joints. The upper part normally slides with the bottom part through the horizontal joint (Tomazevic, 1999). From experiments, the response of the wall with this type of failure mode is very stable and is characterized by high energy dissipation, an elastic perfectly plastic behaviour with large displacement capacity (Salmanpour et al., 2013).

Diagonal shear failure is referred to as shear failure and is considered the typical failure mode for masonry walls subjected to in-plane seismic actions. Diagonal shear failures occur due to an increase of the principal tensile stresses within the wall that supersedes the in-plane tensile capacity of masonry materials. The principal tensile stresses are developed by simultaneous application of vertical and horizontal loads which is responsible to cause diagonal cracks within the wall. The cracks will follow the mortar joints in a stair-case shape or go through the masonry units (Tomazevic, 1999). This type of failure process has resulted in moderate energy dissipation, a rapid loss of strength and stiffness, and a limited displacement capacity in masonry walls. In the case of walls built with poor-quality mortar, diagonal cracks may form along the mortar joints causing a sliding movement of one part of the wall with the other (Salmanpour et al., 2013).

Flexural failure occurs due to an increase in shear capacity and a high moment/shear ratio in the masonry wall. An increase in the horizontal load induces tension cracks in the bed joints resulting in the crushing of masonry units in the compressed zones (Tomazevic, 1999). Walls with the flexural mode of failure have a nonlinear elastic response characterized by moderate energy dissipation and low strength degradation. Significant displacement might occur when the imposed vertical load is less than the compressive strength of masonry (Salmanpour et al., 2013).

Fernando et al. (2015) describe the deformation and failure mode of a masonry structure. The research presented there focused on understanding the mechanical properties of the basic block-mortar set, which is responsible for the wall performance and failure. They conduct an extensive experimental program to access the failure mode and deformation capability of walls. The research concludes that one of the main causes of nonlinearity of masonry is an increase in lateral deformation with increasing loading, which was due to extensive cracking of mortar, a progressive increase in the Poisson's ratio of the structure, and vertical cracks that occurred in the interface of the block-head mortar joint. The data on this research shows that these phenomena happened when the stress on the wall reaches approximately 60% of the ultimate strength.

Magenes and Calvi (1997) studied the in-plane seismic response of brick masonry walls. This paper presents the three principal modes of failure which are: rocking failure, Shear cracking, and sliding. Mechanism of lateral force resistance primarily depends on the pier geometry, boundary condition, the magnitude of vertical load, on the characteristic of the brick, the mortar, and the brick/mortar interface. This Paper state that damage propagates stably and slowly until a sudden and unstable propagate occurs which determines the failure of the wall and initiates the softening of the load-displacement curve. Response of brick masonry wall is nonlinear at the low level of load due to low tensile strength of bed and head joint. Experimental behaviour of simple pier shows that; in case of flexural response like rocking, large displacement without significant loss in strength, moderate hysteretic energy dissipation, and almost nonlinear elastic behaviour are found. In the case of shear-dominated response like diagonal tension failure, the behaviour was characterized by higher energy dissipation, rapid strength, and stiffness degradation.

Abrams (2004) studied the out of the plane response of unreinforced masonry bearing wall with a flexible diaphragm. The intensity of axial load on the wall and the mass of the wall affect out-of-plane response. The collapse occurred for reduced axial load and increased wall mass. An increase in spectral displacement is due to an increase in time period that results from a flexible diaphragm. Diaphragm flexibility significantly increases the out-of-plane displacement and amplified the diaphragm mid-span displacement and acceleration response with respect to the in-plane wall.

2.5 Literature related to modelling of masonry structure

Lourenco et al. (2006) addressed the different homogenization techniques available in the literature. The micro-modeling of the constituent components of masonry might be the focus of the methodology for numerical representation of masonry, viz. units (stone, brick, block, etc.) and mortar, or the macro-modelling of the masonry as a composite. Depending on the level of precision and the simplicity desired, it is possible to use the different modelling strategies for different models.

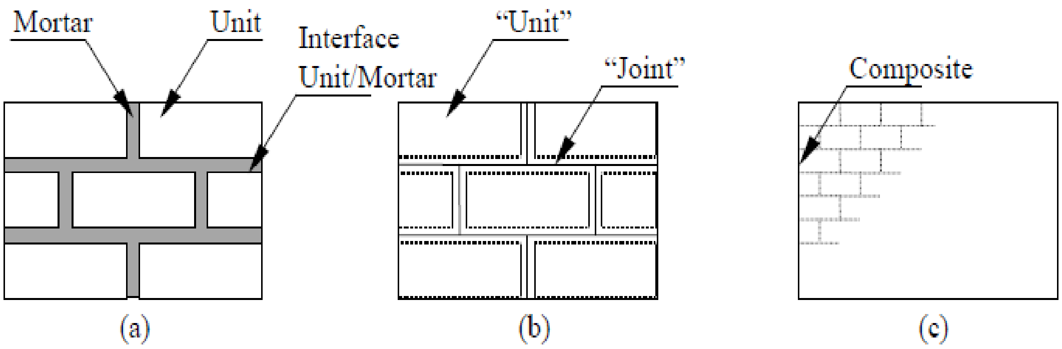

Figure 2-7: Modelling strategies for masonry structures: (a) detailed micro-modelling; (b) simplified micro-modelling; (c) macro-modelling

In detailed micro-modelling of the masonry wall, units and mortar in the joints are represented by continuum elements whereas the unit-mortar interface is represented by discontinuum elements. In Simplified micro-modelling of a masonry wall, expanded units are represented by continuum elements whereas the behaviour of the mortar joints and the unit-mortar interface is lumped in discontinuum elements. Similarly in Macro-modelling units, mortar, and unit-mortar interfaces are smeared out in a homogeneous continuum.

Poisson's ratio, Young's modulus, and optionally, inelastic properties of both unit and mortar of masonry are considered in the micro modelling approach of the masonry wall. The interface in this modelling approach represents a potential crack/slip plane with initial dummy stiffness to avoid interpenetration of the continuum. This enables us to study the combined action of unit, mortar, and interface under a magnifying glass. Each joint consisting of mortar and the two unit-mortar interfaces is lumped into an average interface in the simplified micro-modeling technique, while the units are extended to maintain the geometry unchanged. Masonry is viewed as a collection of elastic blocks held together by potential fracture/slip lines at the joints in this method.. Accuracy is lost in this method since Poisson's effect on the mortar is not included. In the macro modelling approach, Masonry is treated as a homogeneous anisotropic continuum and does not make the distinction between individual units and joints. One strategy of masonry models cannot be used over the other because different application fields exist for the different strategies of models. To understand the detail and local behaviour of masonry structures study of micro-modelling is necessary.

Dejong et. al. (2009) implemented shell elements into the sequentially linear analysis method. The study was aimed to model three dimensional masonry structures under non-proportional loading. At first shell element implementation is presented and then it was applied to simulate two previous full-scale experimental tests on unreinforced masonry structure through wider cyclic loading. In this study three dimensional failure mechanisms were effectively predicted, provided that further evidence to support sequentially linear analysis as an alternative method to non-linear analysis in the finite element framework They conclude that three-dimensional failure can be directly predicted in shell elements that eliminate the need to estimate the participating area of perpendicular walls when modelling in two dimensions.

Colunga and Abrams (1996) studied the influence of floor flexibility on the seismic response of building structures. They compare the computed seismic response for flexible diaphragm structures and equivalent structures with rigid diaphragms. They illustrated the difference in the flexible diaphragm and rigid diaphragm through the case studies of three existing buildings with flexible diaphragms and analogous systems with rigid diaphragms. The paper discusses that structures with flexible diaphragms can experience higher accelerations and displacements than structures with rigid diaphragms, and also their fundamental periods of vibration can be significantly longer in flexible diaphragms.

Cardoso et al. (2005) In the modeling of a masonry wall, it was difficult to select the method that truly represents the masonry wall. A commercial software SAP2000 was used for modelling of masonry. In this paper, shell modeling with equivalent timber floor has been used. They presented a three-dimensional timber structure enclosed in a masonry wall aimed at providing seismic resistance features. Thin bi-dimensional shell elements were used to model the exterior wall of masonry considering only bending deformation. Timber elements were considered for the interior walls. Timber elements were simulated by bars that transmit only axial forces. Rotations are free at the connections. They conclude that experimental and numerical stiffness would be similar if, in the numerical model, masonry elements were removed and the connections of diagonal elements under tension were not considered.

This research concludes that it was not worth refining the mesh for masonry elements more, bearing in mind that the level of accuracy does not need to go beyond the accuracy in the evaluation of the material properties as input. Furthermore, the primary goal of analyzing crack/crush in masonry elements was to determine the extent and location of masonry damage, as this is crucial in determining the type of collapse mechanism.

The floors were designed as truss bars with free rotations at the wall connections, imitating flexible plane relative displacement of parallel walls. In this paper the connections between timber elements of the ‘gaiola’ and perpendicular masonry walls were simulated considering short bars that only resist axial forces, intending to simulate the strength of the connection. In the evaluation of the strength of the connection, no iron elements were considered due to the uncertainties about their real existence in the buildings.

Maharjan and Parajuli (2020) evaluated the newly built stone masonry house at chautara municipality, Sindupalchowk with mud mortar and with the provision of horizontal reinforced concrete (R.C.) bands. To investigate the seismic performance of stone masonry houses, structures with different geometry and RC bands were selected modelled, and analyzed. The stone masonry wall has been built with stone with mud mortar, was modelled with shell elements.

Two typical houses of masonry houses with wall thickness 18" were modelled by SAP 2000 version 19. The rectangular shell element was considered for the model of the masonry wall. The partition walls of selected masonry buildings were also considered as shell elements during the modeling. The base of the masonry building is made fixed.

A vertical reinforcing bar and a plinth band were included in the construction of the dwellings. Horizontal RC bands with a three-inch thickness of masonry building were modeled as a frame element. Vertical bars used in the building were modeled as a frame element (12mm dia) and designed sections with solid sections. The opening frames, rafter, battens, ridge, joists, timber beam, and roof post of the building were modeled as frame elements and designed sections with solid sections. For modeling of the timber floor, a three-dimensional linear beam element was used to model the timber beam. The connection of the timber floor with the masonry wall was assumed that it was simply resting on the masonry wall. So, a simply supported connection was used for modeling the joint between the timber beam and the masonry wall of a building.

2.6 Literature Related to Dynamic Analysis and Fragility Analysis

Sucuoglu and Erberik (1997) performed the dynamic analysis of a three-storey masonry building that survived during the 1992 Erzincan earthquake without damage. In this research mechanical properties of masonry wall was found experimentally by using the identical brick and mortar that are used for construction of building structure. The material model is developed for masonry structure and employed in a computer program for the non-linear dynamic analysis of masonry buildings. The result of this research shows that the masonry structure which satisfies basic seismic code requirements has remarkable lateral strength, stiffness, and energy dissipation capacity. They conclude that masonry buildings have the advantages of remarkably high lateral resistance capacity and stiffness when they are constructed even with the minimum material quality required by the seismic design codes. A uniform distribution of shear stresses can easily be achieved if a regular plan geometry is adopted.

Benedetti and Castellani (1980) tested physical models of masonry structures at the Politecnico of Milan. At first, they discussed about meaningfulness of a static approach for seismic studies. A nonlinear dynamic numerical model is worked out. They found that, in general, a dynamic approach offers greater margins of safety than a static approach. They experience that, the greater portion of damage or collapse of masonry structures during violent earthquakes can be attributed to poor linkage between orthogonal walls; or to lack of rigid slabs; or to inappropriate roofs; or to settlement of foundations; or to adjacent structures hammering; or to poor materials.

Magenes et al. (2013) conducted an experimental campaign to understand the dynamic behavior of historic stone masonry structures and evaluate the seismic performance of selected strengthening strategies, aimed at improving wall-to-floor connections and in-plane diaphragm stiffness. Shaking table tests were performed of full-scaled masonry building with timber floor and roof. Two buildings were tested in this research in which a first prototype, representing a vulnerable building without seismic detailing, was tested showing a response characterized by in-plane distortion of the flexible diaphragms and local out-of-plane failure mechanisms. In the second Building the wall-to-diaphragm connections were improved, providing only a moderate in-plane stiffening of the wooden diaphragms. Both buildings were subjected to shake-table testing, the strengthened building showed a global type of structural response without the occurrence of out-of-plane mechanisms. In this paper the strengthening interventions on Building II are described, and the results obtained during the dynamic tests are illustrated. They found that improvement of the connections proved to be very effective, increasing significantly the seismic capacity of the Building.

Bakhshi and Karimi (2008) studied a fragility curve for different types of a masonry building. Different state of damage occurs when the building is subjected to a different type of earthquake. In this paper, five damage states were considered. They are Nonstructural damage, Slight structural damage, Moderate structural damage, Severe structural damage, and Collapse. For the most probable earthquakes, which are the ones with moderate intensity (0.2 g < PGA < 0:5 g) following results were concluded.

- Nonstructural and slight damage occurs and moderate damage is, therefore, probable in one-story unreinforced masonry buildings without ties. In this type of building, the probability of occurring severe damage is, approximately, 35% and the probability of collapse is less than 20%.
- Nonstructural, slight and moderate damage states are completely possible in three-story unreinforced masonry buildings without ties. In this type of building, the probability of occurring severe damage is more than 60% and the probability of collapse is between 30% and 45%.
- The probability of each state of damage occurring is negligible in one storey reinforced masonry buildings.

Colangelo (2008) a number of approaches to derive seismic fragility curves have been mentioned and applied to a single in filled-frame structure. The resulting fragility curves from different approaches are compared empirically. In this research damage of the nonstructural infill wall was considered, in correlation with the peak inter-story drift ratio and depending on the PGA. The research reveals that if a threshold drift value is connected with the incidence of damage, then the fragility increases dramatically with the PGA, and if the lower bound of a range of probable drift values is used, then the fragility is exaggerated to a conservative degree.

Rota et al. (2008) gives a new analytical approach for the derivation of fragility curves for masonry buildings. This study's methodology is based on nonlinear stochastic analysis of construction prototypes. Because masonry constructions are supposed to be representative of a wider range of typologies, the model's mechanical properties are treated as random variables that should fluctuate within reasonable limits.
After that Monte Carlo simulations are used to generate input variables from the probability density functions of mechanical parameters. Nonlinear analysis are performed once the model is defined. Nonlinear static (pushover) analyses, in particular, are used to define the probability distributions of each damage condition, whereas nonlinear dynamic analyses are used to determine the probability density function of the displacement demand corresponding to various amounts of ground motion.

HAZUS 4.2 SP3 (2020) is an earthquake model technical manual. It was designed to develop plans for recovery and reconstruction resulting from disaster and mitigating the possible consequences of earthquakes. In this technical manual, four damage states are defined for building structural system components which are slight, moderate, extensive, and complete. The PEH (Potential Earthquake Hazards) demand parameter's median value defines each fragility curve (i.e., either spectral displacement, spectral acceleration, PGA, or PGD).

The conditional probability of being in, or exceeding, a particular damage state given the spectral displacement, S_d, (or other PEH parameter) is defined by the function:

$$p[ds|\mathrm{Sd}] = \phi[\frac{1}{\beta ds}\ln\left(\frac{Sd}{Sd,ds}\right)]$$

Where:

$S_{d,ds}$ is the median value of spectral displacement at which the building reaches the threshold of the damage state, d_s.

β_{ds} is the standard deviation of the natural logarithm of spectral displacement for damage state, d_s, and

ϕ is the standard normal cumulative distribution function.

The total inconsistency of each equivalent-PGA, β_{SPGA} is modelled by the combination of two contributors to damage variability. Uncertainty in the damage-state threshold of the structural system ($\beta_{M(SPGA)}$=0.4 for all building types and damage states) and Variability in response due to the spatial variability of ground motion demand ($\beta_{D(V)}$ = 0.5 for long-period spectral response).

The two contributors to damage state variability are assumed to be log-normally distributed, independent random variables and the total variability is simply the square-root-sum-of-the-squares combination of individual variability terms. Summarize the median and lognormal standard deviation (SPGA) values for the PGA-based structural damage states of Slight, Moderate, Extensive, and Complete. For masonry structure, β_{SPGA} can be extracted from table 5-29 HAZUS 4.2 SP3 and is equal to 0.64.

3 MODELLING AND ANALYSIS

3.1 General

Four building typologies suitable for rural areas of Nepal are considered (HRRP, 2018). The different building typologies are modelled in SAP 2000V.22. and are subjected to earthquake loadings. The building will undergo certain deformation when subjected to an earthquake load. Response of building for lateral load is directly proportional to the stiffness of the building. During an earthquake, buildings experience several types of damage, but in this study, the damage is idealized as the maximum top storey displacement of each building. This is because that the structures are all designed for ductility under seismic loads and so deformations are more meaningful than forces (Tremayne and Trevor 2005).

3.2 Building Description

Four building typologies with a similar plan are considered. The usable space of the building is constant where the thickness of the wall is different according to NBC-202 (2015), NBC-203 (2015). The detailed description of building typology considered in this research are:

• Brick masonry with Cement mortar (BCEM)

• Stone masonry with Cement mortar (SCEM)

• Stone masonry with mud mortar (SMUD)

• Cement mortar CSEB blocks (CSEB)

Table 3-1: Building Description of different typology

Building Type	Length (m)	Breadth (m)	Wall Thickness(mm)	Floor Height m	No. of Floor
BCEM	8.72	4.56	230	2.75	2
SCEM	9.2	4.8	350	2.75	2
SMUD	9.6	4.9	450	2.75	2
CSEB	8.76	4.58	240	2.75	2

3.3 Modelling - Macro Element Modelling

The macro-element model does not make a distinction between individual units and joints but treats masonry as a homogeneous anisotropic continuum (Lourenco et. al., 2006). This model is a macroscopic representation of a continuous model in which the parameters are directly correlated to the mechanical properties of the masonry elements

(Gambarotta and Lagomarsino 1997). The macro-element parameters of masonry should be considered as representative of the average behavior of the masonry panel. The 3-dimensional building models are simulated by joining the masonry walls together. Masonry walls are simulated by thin bi-dimensional elements (shell elements) considering only in-plane behavior. The wall's out-of-plane bending/shear response is not computed because it is considered negligible with respect to the global building response (Ilaria 2010).

For modeling of the timber floor element, a three-dimensional linear beam element is used to model the timber beam. The connection of the timber floor/roof with the masonry wall was assumed that it was simply resting on the wall. The base of the masonry houses is made fixed. Horizontal bands are modeled as a frame element. Vertical bars used in the building were modeled as a frame element and designed sections with solid sections. The opening frames, rafter, battens, ridge, joists, timber beam, and roof post were modeled as frame elements and designed sections with solid sections. The detailed description of different frame elements as per NBC 202-2015 and NBC 203-2015 are:

Table 3-2: Section size of different element

S.N	Element	Size
1	Timber Floor Beam	240mm*120mm
2	Band	75mm*wall thickness
3	Rafter/Purlin	120mm*65mm
4	Roof Post	120mm Φ
5	Ridge Beam	120mm*65mm
6	Vertical Reinforcement	12mm Φ

3.4 The materials properties for the analysis

For Brick masonry with Cement mortar (Phaiju and Pradhan, 2020)

Young’s modulus (E_m) = 2703.2 N/mm^2

Shear modulus (G) = 915.1 N/mm^2

Poisson’s ratio (ν) = 0.32

Unit weight (Υ) = 18.85 KN/m^3

For coursed stone masonry cement mortar (Magenes et. al., 2010)

Young's modulus (E_m) = 2550 N/mm^2

Shear modulus (G) = 840 N/mm^2

Poisson's ratio (ν) = 0.25

Unit weight (ϒ) = 22 KN/m3

For Coursed Stone Masonry with mud mortar (Meimaroglou and Mouzakis, 2018)

Young's modulus (E_m) = 502.19 N/mm^2

Shear modulus (G) = 209.2 N/mm^2

Poisson's ratio (ν) = 0.2

Unit weight (ϒ) = 17 KN/m^3

For CSEB (Mellegard and Steinert, 2016)

Young's modulus (E_m) = 851 N/mm^2

Shear modulus (G) = 354 N/mm^2

Poisson's ratio (ν) = 0.2

Unit weight (ϒ) = 17.65 KN/m^3

For timber (IS 883: 1994)

Weight per unit volume (ϒ) = 8.05 KN/m^3

Modulus of elasticity (E) = 12600 N/mm^2

Poisson ratio =0.12

For Bamboo (IS 883: 1994)

Weight per unit volume (ϒ) = 6.602 KN/m^3

Modulus of elasticity (E) = 10720 N/mm^2

Poisson ratio =0.12

Gravity load was calculated based on the unit weight of the material and live load was taken as 2KN/m^2. The roof load depends on what type of roofing is used. Approximate calculations suggest a roof load equal to 1.5 KN/m^2 which represents a thin slate roof, corrugated galvanized iron (CGI) sheets, or thick rammed earth (Parajuli, 2016). Models were designed using SAP 2000 V 22. The plan of building and model for the analysis are shown in Figures 3-1 and 3-2.

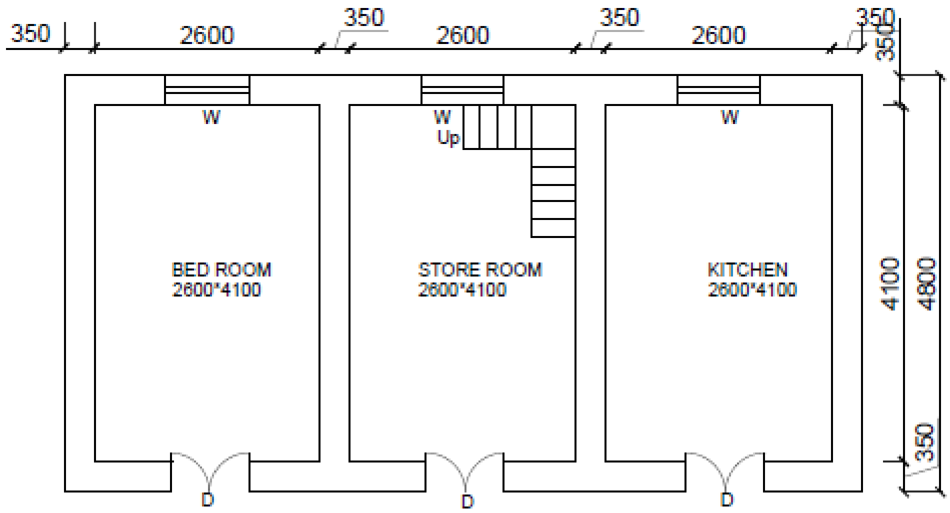

Figure 3-1: Ground floor Plan of SCEM Building

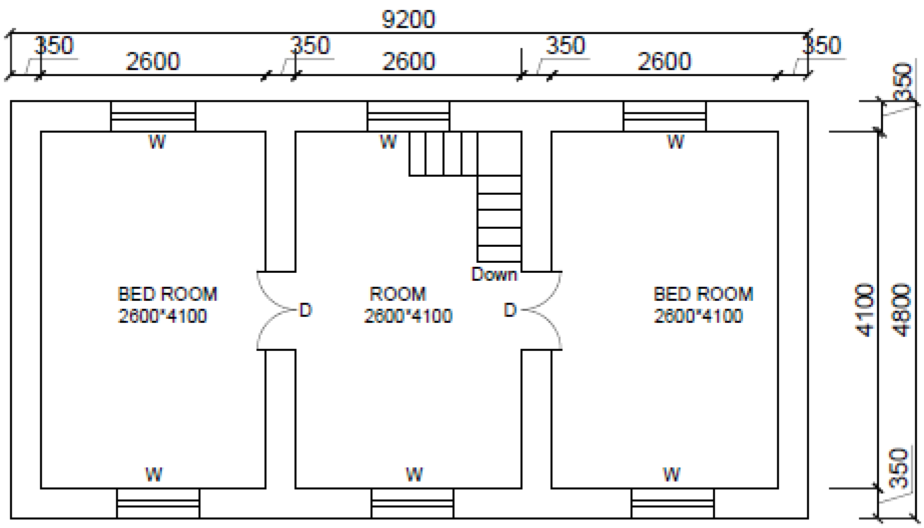

Figure 3-2: First floor Plan of SCEM Building

The Plan and elevation of different typologies (BCEM, SMUD, CSEB) are same. The material properties and wall thickness of these typologies are different as mention above.

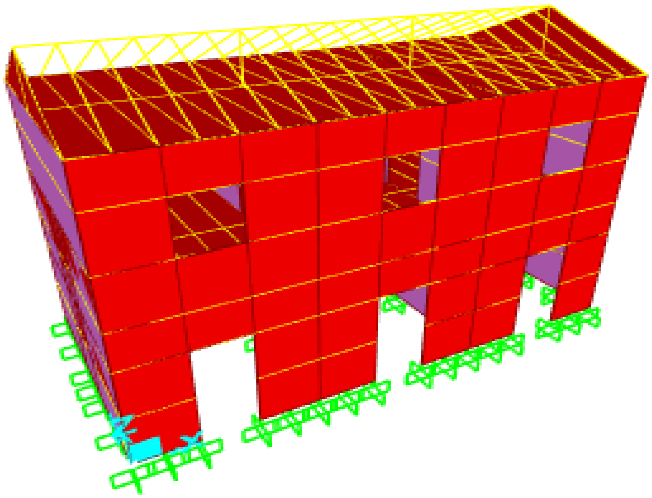

Figure 3-3: Model of SCEM in SAP2000

3.5 Method of Analysis

The four methods of analysis to analyze any structural problem are:

- Linear static analysis
- Linear Dynamic analysis
- Nonlinear static analysis
- Nonlinear Dynamic analysis

The starting point for understanding the behaviour of masonry structures can be a linear elastic analysis under the assumption of masonry as a homogenous material (Ilaria 2010). After the completion of modelling in SAP 2000 V22, modal analysis was carried out. Linear time history analysis was carried out for different earthquakes with scaling PGA. Since a single record is not sufficient to describe the behaviour of the structure, a sufficient number of records is required (Bommer and Beyer 2007).

Seismic Input

Ground motion parameters may be acceleration, velocity or Displacement or all three combined together. The acceleration is usually the directly measured quantity, while the other characteristics are derived from acceleration. Due to technical incapability and instrumental setup for recording accurate earthquake, so there is no actual record of earthquake data. Therefore, the ground motions assumed for use in this research are synthetic earthquake that consists of a simulated ground motions time history of Gorkha, Imperial Valley and Kobe.

In order to carry out dynamic analyses, an appropriate set of acceleration time histories is required (Bommer et. al., 2003). The three records considered in this study were scaled linearly to the required PGA. The PGA has been rescaled to 0.2g, 0.3g, 0.45g, 0.6g, 0.75g, 0.9g and 1g. The three accelerograms peak amplitudes are given in Table, and the records are shown in Figure.

S.N	Name of EQ	PGA
1	Gorkha	0.1634g
2	Imp Valley 1940	0.2808g
3	Kobe	0.3447g

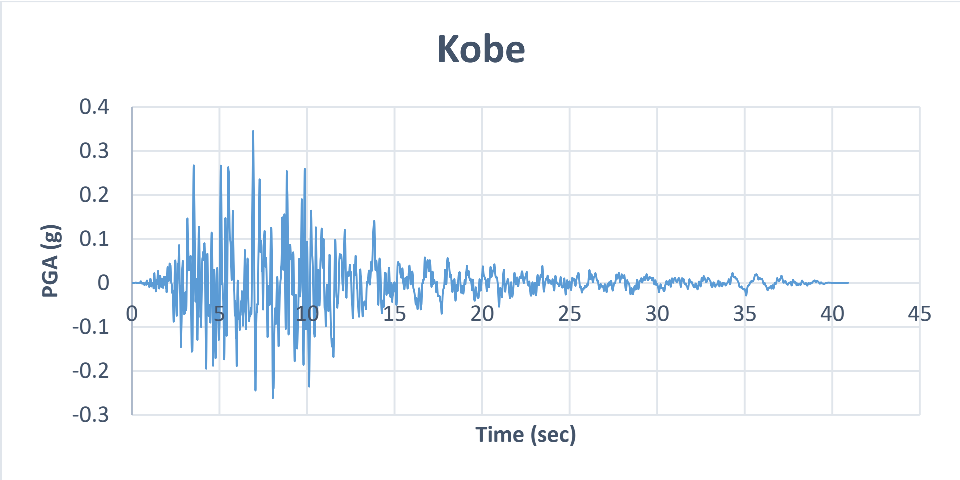

Figure 3-4: Time history graph of Kobe

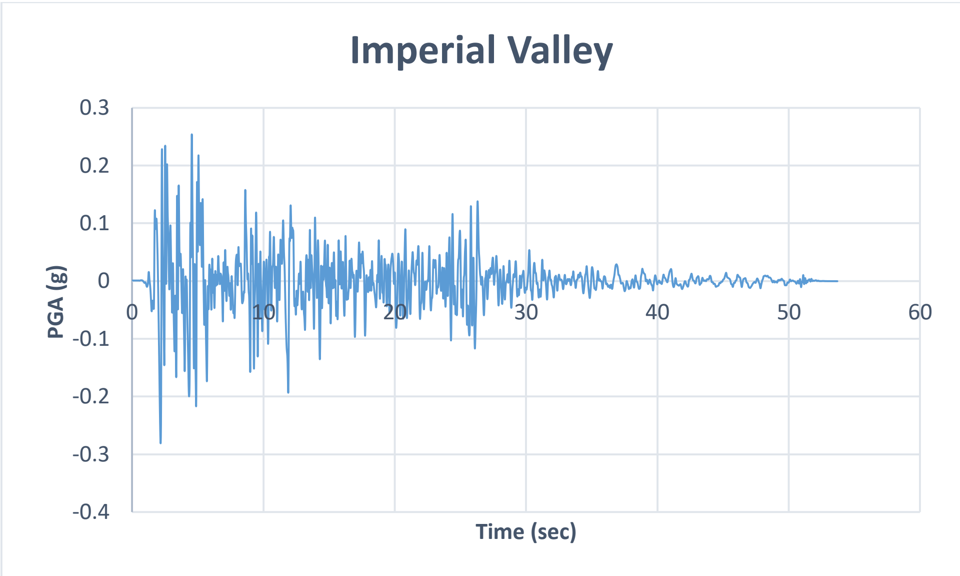

Figure 3-5: Time History graph of Imperial Valley 1940

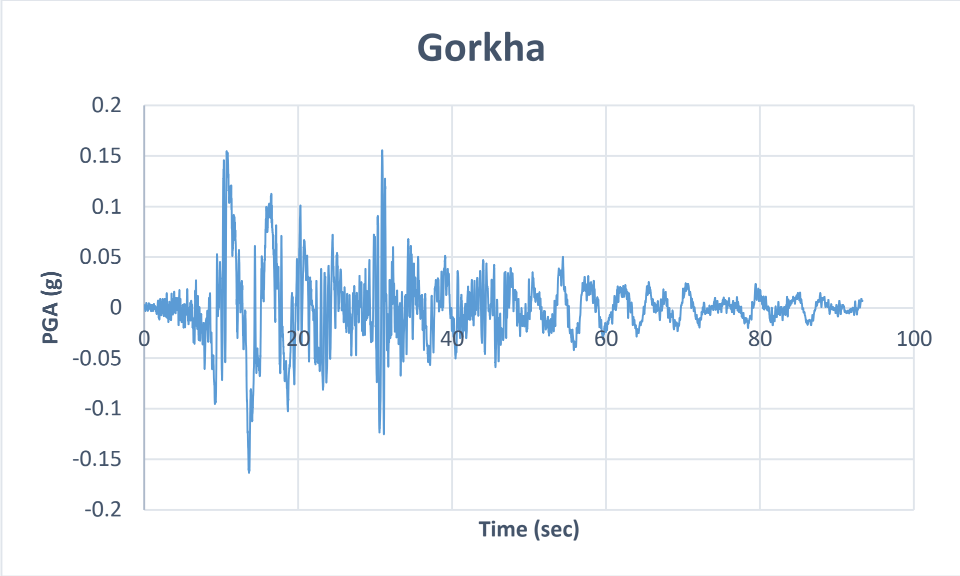

Figure 3-6: Time History graph of Gorkha Earthquake

Modal Analysis

Modal analysis is used to determine the vibration mode of a structure to understand the dynamic behaviour of a structure. The two types of modal analysis are Eigenvector and Ritz vector analysis. The system undamped free vibration mode forms and frequencies are determined via eigenvector analysis.

Eigenvector analysis provides the solution to the general Eigenvalue problem.

$\big[[K] - w^2[M]\big]\{\emptyset\} = \{0\}$ (Clough and Penzien, 2003)

Where [K] is the stiffness matrix

[M]- diagonal mass matrix

w^2- Matrix of a square of corresponding Eigen values

$\{\emptyset\}$- Matrix of corresponding Eigen vector mode shapes

The cyclic frequency and the time period are related by

$T=\frac{1}{f}$

$f= \frac{w}{2\Pi}$

Dynamic analysis-Time History Analysis

If loads or displacements are delivered slowly enough, inertia forces can be ignored and static load analysis justified; otherwise, dynamic structural analysis is required. The dynamic equilibrium equation is a second-order differential equation is given by

$$[M]\{\ddot{X}(t)\}+[C]\{\dot{X}(t)\}+[K]\{X(t)\}=\{F(t)\}$$

For seismic loading, the external loading $\{F(t)\}$ is zero. The basic seismic motions are the three components of free field ground accelerations that are known at the surface where the foundation is laid.

$$[M]\{\ddot{X}(t)\}+[C]\{\dot{X}(t)\}+[K]\{X(t)\}=-[M]_x\{\ddot{X}(t)\}_{xg}-[M]_y\{\ddot{X}(t)\}_{yg}-[M]_z\{\ddot{X}(t)\}_{zg}$$

A time history analysis is a step-by-step assessment of a structure's dynamic reaction to a defined loading that may change over time.

Fragility Analysis

Building fragility curves express the probability of a building reaching or exceeding a certain damage state for a given ground motion parameter. Fragility curve methodologies using analytical approaches have become widely adopted because they are more readily applied to structures. For seismic loading, the fragility simply examines the probability that the seismic demand exerted on the structure (D) exceeds the structure's capacity (C).

Damage evaluation will be carried out using the fragility function that is given as lognormal distribution in which a spectral displacement is applied as a stochastic variable. A basic equation is

$$Pf = \emptyset\left(\frac{ln\left(\frac{S_d}{S_c}\right)}{\beta}\right)$$

Where Pf is the probability of failure

ϕ( ) is the Operational calculus for obtaining the cumulative standard normal distribution function

S_d and S_c are demand and capacity displacement

β is the log standard deviation that represents total uncertainty. It's a prediction that takes into consideration various unknown elements that affect the reliability of the functions and have an impact on determining the median PGA in the fragility curves derivation process. It is simply the combination of the square root sum of the square of individual variability terms which is equivalent to 0.64.

In HAZUS 4.2 SP3 (2020) there are four damage states: Slight, Moderate, Extensive, and Complete. Spectral displacement are used to describe structural limit states. In this research damage states from HAZUS is adopted according to its assumption that the total variability of each equivalent-PGA structural damage state, β_{SPGA}, is modeled by the combination of the following two contributors to damage variability, uncertainty in the damage-state $\beta_{M(SPGA)}$ = 0.4 and variability in response $\beta_{D(V)}$ = 0.5. The two contributors to damage state variability are assumed to be log-normally distributed, independent random variables and the total variability is simply the square-root-sum-of-the-squares combination of individual variability terms β_{SPGA} =0.64 for all damage states (Slight, Moderate, Extensive and Complete damage).

Four damage states are used as the capacity of the building (GIovinazzi et al., 2006)

Slight =0.7d_y , Moderate =1.5d_y , Extensive =0.5(d_y+d_u),Complete =d_u

Where,

d_y = yield displacement =0.16 inch

d_u = Ultimate displacement =1.598inch , (HAZUS, 2020).

4 RESULT AND DISCUSSION

4.1 General

The four representative buildings were modeled in SAP 2000V22 using the finite element modeling concept. Then Modal and linear time history analysis was performed for the response of the selected buildings. These four buildings are of different mechanical properties and wall thickness but all of them have common usable space. The results were in terms of maximum (top) displacements and base shear. The fragility curves of each building with four damage states namely slight, moderate, extensive, and complete for three earthquakes: Gorkha, Imp valley, and Kobe are demonstrated. These are derived from the response and capacity analysis of the buildings.

From the free vibration analysis (model) fundamental time periods for building BCEM, SCEM, SMUD and CSEB are 0.143, 0.146, 0.175 and 0.168sec respectively for the first mode. Linear time history analysis was applied for the dynamic response of the sample buildings. For this response analysis, three earthquakes were taken in the form of ground motion time history as seismic input with different intensities. The responses of buildings in terms of top displacements show that the Kobe earthquake produces more displacement compared to Gorkha and Imp Valley earthquake.

4.2 Displacement

The displacement of different typology for three earthquakes are shown in table 4-1 to 4-12. Lateral displacement of BCEM typology at PGA 0.4g for Gorkha, Imp Valley and Kobe earthquake was 2.462mm, 3.242mm and 5.219mm. Lateral displacement of SCEM typology at PGA 0.4g for Gorkha, Imp Valley and Kobe earthquake is 3.281mm, 6.034mm and 7.231mm. Similarly, Lateral displacement of SMUD typology at PGA 0.4g for Gorkha, Imp Valley and Kobe earthquake is 5.786mm, 10.455mm and 12.020mm. Lateral displacement of CSEB typology at PGA 0.4g for Gorkha, Imp Valley and Kobe earthquake is 3.962mm, 7.497mm and 10.809mm. Similarly displacement and drift at different PGA for each earthquake and typologies were determined.

4.3 Base shear

The base shear of different typology for three earthquakes are shown in table 4-1 to 4-12. The figure 4-1 and 4-2 shows that base shear of all four typologies of building varies linearly with an increase in PGA (g). This is due to linear time history has shown all parameters vary linearly along with Sa/g (Maharjan and Parajuli, 2020). The base shear of SMUD typology is highest among the four typologies and the base shear of BCEM typology is lowest among four typologies.

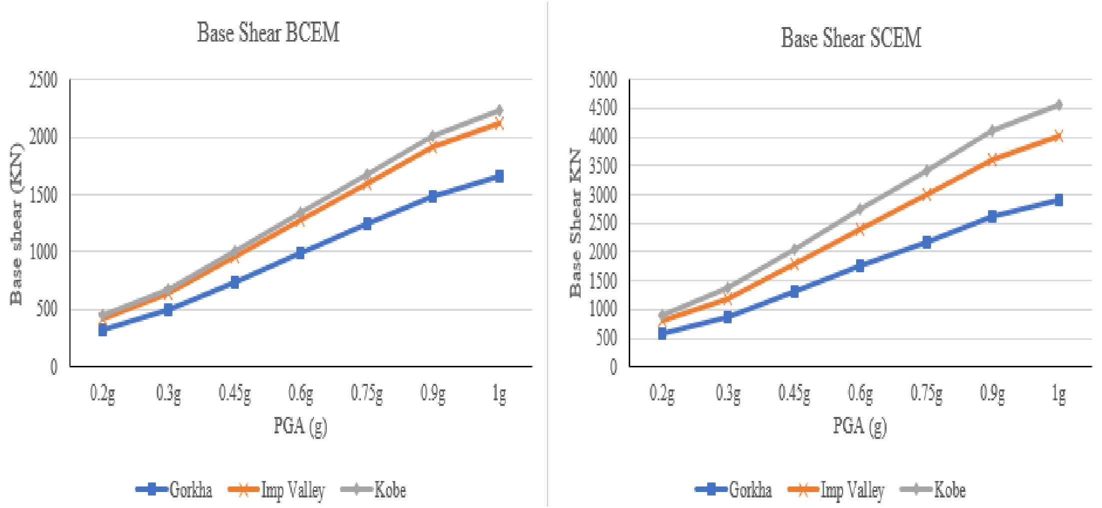

Figure 4-1: Comparison of base shear for different earthquake (BCEM and SCEM) typology

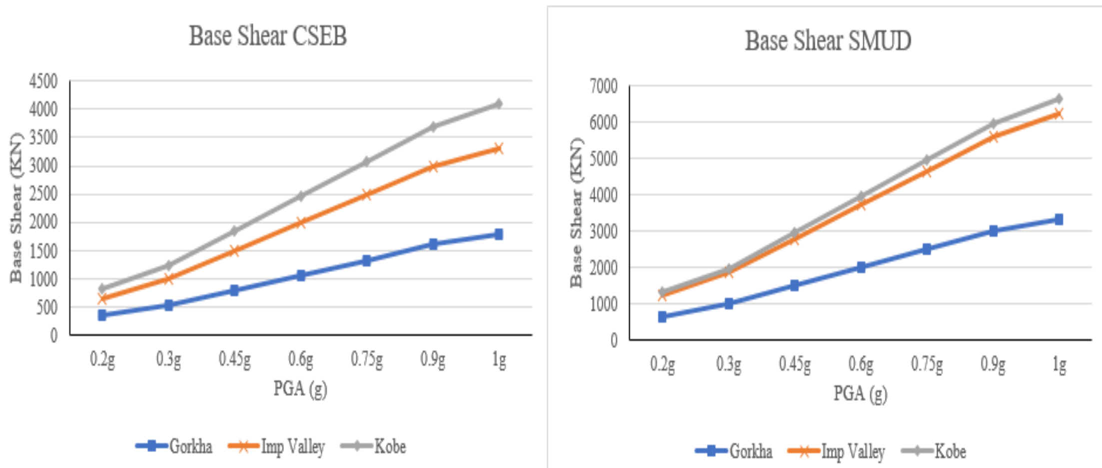

Figure 4-2: Comparison of base shear for different earthquake (CSEB and SMUD) typology

4.4 Fragility analysis

The calculation for the development of the fragility curve of the four representative sample buildings is presented in table 4-13 to 4-24 and figure 4-3 to 4-14 shows the fragility curves, which shows the probability of failure for different intensities of earthquake (PGA) as seismic input of Gorkha, Imp Valley and Kobe earthquake with different damage state slight, moderate, extensive and collapse.

Table 4-1: Response of BCEM Building (Gorkha)

Gorkha Earthquake (BCEM), PGA = 0.2g				
Storey Level	Storey height (m)	Displacement (mm)	Drift (%)	Base Shear (KN)
Ground level	0	0	0	330.973
First Floor	2.75	0.979	0.036	
Second Floor	5.5	1.231	0.009	
PGA = 0.3g				
Storey Level	Storey height (m)	Displacement (mm)	Drift (%)	Base Shear (KN)
Ground level	0	0	0	496.460
First Floor	2.75	1.468	0.053	
Second Floor	5.5	1.847	0.014	
PGA = 0.45g				
Storey Level	Storey height (m)	Displacement (mm)	Drift (%)	Base Shear (KN)
Ground level	0	0	0	744.690
First Floor	2.75	2.202	0.080	
Second Floor	5.5	2.770	0.021	
PGA = 0.6g				
Storey Level	Storey height (m)	Displacement (mm)	Drift (%)	Base Shear (KN)
Ground level	0	0	0	992.920
First Floor	2.75	2.936	0.107	
Second Floor	5.5	3.693	0.028	
PGA = 0.75g				
Storey Level	Storey height (m)	Displacement (mm)	Drift (%)	Base Shear (KN)
Ground level	0	0	0	1241.149
First Floor	2.75	3.670	0.133	
Second Floor	5.5	4.617	0.034	
PGA = 0.9g				
Storey Level	Storey height (m)	Displacement (mm)	Drift (%)	Base Shear (KN)
Ground level	0	0	0	1489.379
First Floor	2.75	4.404	0.160	
Second Floor	5.5	5.540	0.041	
PGA = 1.0g				
Storey Level	Storey height (m)	Displacement (mm)	Drift (%)	Base Shear (KN)
Ground level	0	0	0	1654.866
First Floor	2.75	4.894	0.178	
Second Floor	5.5	6.156	0.046	

Table 4-2: Response of BCEM Building (Imp Valley)

Imp Valley Earthquake (BCEM), PGA = 0.2g				
Storey Level	Storey height (m)	Displacement (mm)	Drift (%)	Base Shear (KN)
Ground level	0	0	0	446.886
First Floor	2.75	1.126	0.041	
Second Floor	5.50	1.620	0.018	
PGA = 0.3g				
Storey Level	Storey height (m)	Displacement (mm)	Drift (%)	Base Shear (KN)
Ground level	0	0	0	670.970
First Floor	2.75	1.691	0.061	
Second Floor	5.5	2.432	0.027	
PGA = 0.45g				
Storey Level	Storey height (m)	Displacement (mm)	Drift (%)	Base Shear (KN)
Ground level	0	0	0	1006.455
First Floor	2.75	2.537	0.092	
Second Floor	5.5	3.648	0.040	
PGA = 0.6g				
Storey Level	Storey height (m)	Displacement (mm)	Drift (%)	Base Shear (KN)
Ground level	0	0	0	1341.939
First Floor	2.75	3.382	0.123	
Second Floor	5.5	4.864	0.054	
PGA = 0.75g				
Storey Level	Storey height (m)	Displacement (mm)	Drift (%)	Base Shear (KN)
Ground level	0	0	0	1677.552
First Floor	2.75	4.228	0.154	
Second Floor	5.5	6.081	0.067	
PGA = 0.9g				
Storey Level	Storey height (m)	Displacement (mm)	Drift (%)	Base Shear (KN)
Ground level	0	0	0	2012.909
First Floor	2.75	5.074	0.184	
Second Floor	5.5	7.296	0.081	
PGA = 1.0g				
Storey Level	Storey height (m)	Displacement (mm)	Drift (%)	Base Shear (KN)
Ground level	0	0	0	2236.992
First Floor	2.75	5.638	0.205	
Second Floor	5.5	8.109	0.090	

Table 4-3: Response of BCEM building (Kobe)

Kobe Earthquake (BCEM), PGA = 0.2g				
Storey Level	Storey height (m)	Displacement (mm)	Drift (%)	Base Shear (KN)
Ground level	0	0	0	424.261
First Floor	2.75	1.345	0.049	
Second Floor	5.50	2.609	0.046	
PGA = 0.3g				
Storey Level	Storey height (m)	Displacement (mm)	Drift (%)	Base Shear (KN)
Ground level	0	0	0	636.391
First Floor	2.75	2.017	0.073	
Second Floor	5.5	3.914	0.069	
PGA = 0.45g				
Storey Level	Storey height (m)	Displacement (mm)	Drift (%)	Base Shear (KN)
Ground level	0	0	0	954.512
First Floor	2.75	3.026	0.110	
Second Floor	5.5	5.871	0.103	
PGA = 0.6g				
Storey Level	Storey height (m)	Displacement (mm)	Drift (%)	Base Shear (KN)
Ground level	0	0	0	1272.708
First Floor	2.75	4.034	0.147	
Second Floor	5.5	7.828	0.138	
PGA = 0.75g				
Storey Level	Storey height (m)	Displacement (mm)	Drift (%)	Base Shear (KN)
Ground level	0	0	0	1590.903
First Floor	2.75	5.043	0.183	
Second Floor	5.5	9.785	0.172	
PGA = 0.9g				
Storey Level	Storey height (m)	Displacement (mm)	Drift (%)	Base Shear (KN)
Ground level	0	0	0	1909.099
First Floor	2.75	6.052	0.220	
Second Floor	5.5	11.742	0.207	
PGA = 1.0g				
Storey Level	Storey height (m)	Displacement (mm)	Drift (%)	Base Shear (KN)
Ground level	0	0	0	2121.229
First Floor	2.75	6.724	0.245	
Second Floor	5.5	13.047	0.230	

Table 4-4: Response of SCEM Building (Gorkha)

Gorkha Earthquake (SCEM), PGA = 0.2g				
Storey Level	Storey height (m)	Displacement (mm)	Drift (%)	Base Shear (KN)
Ground level	0	0	0	581.915
First Floor	2.75	1.062	0.039	
Second Floor	5.5	1.640	0.021	
PGA = 0.3g				
Storey Level	Storey height (m)	Displacement (mm)	Drift (%)	Base Shear (KN)
Ground level	0	0	0	872.873
First Floor	2.75	1.593	0.058	
Second Floor	5.5	2.461	0.032	
PGA = 0.45g				
Storey Level	Storey height (m)	Displacement (mm)	Drift (%)	Base Shear (KN)
Ground level	0	0	0	1309.310
First Floor	2.75	2.389	0.087	
Second Floor	5.5	3.691	0.047	
PGA = 0.6g				
Storey Level	Storey height (m)	Displacement (mm)	Drift (%)	Base Shear (KN)
Ground level	0	0	0	1745.746
First Floor	2.75	3.185	0.116	
Second Floor	5.5	4.921	0.063	
PGA = 0.75g				
Storey Level	Storey height (m)	Displacement (mm)	Drift (%)	Base Shear (KN)
Ground level	0	0	0	2182.183
First Floor	2.75	3.981	0.145	
Second Floor	5.5	6.152	0.079	
PGA = 0.9g				
Storey Level	Storey height (m)	Displacement (mm)	Drift (%)	Base Shear (KN)
Ground level	0	0	0	2618.619
First Floor	2.75	4.778	0.174	
Second Floor	5.5	7.382	0.095	
PGA = 1.0g				
Storey Level	Storey height (m)	Displacement (mm)	Drift (%)	Base Shear (KN)
Ground level	0	0	0	2909.577
First Floor	2.75	5.308	0.193	
Second Floor	5.5	8.202	0.105	

Table 4-5: Response of SCEM Building (Imp Valley)

Imp Valley Earthquake (SCEM), PGA = 0.2g				
Storey Level	Storey height (m)	Displacement (mm)	Drift (%)	Base Shear (KN)
Ground level	0	0	0	800.653
First Floor	2.75	1.547	0.056	
Second Floor	5.50	3.013	0.053	
PGA = 0.3g				
Storey Level	Storey height (m)	Displacement (mm)	Drift (%)	Base Shear (KN)
Ground level	0	0	0	1202.126
First Floor	2.75	2.323	0.084	
Second Floor	5.5	4.524	0.080	
PGA = 0.45g				
Storey Level	Storey height (m)	Displacement (mm)	Drift (%)	Base Shear (KN)
Ground level	0	0	0	1803.189
First Floor	2.75	3.485	0.127	
Second Floor	5.5	6.787	0.120	
PGA = 0.6g				
Storey Level	Storey height (m)	Displacement (mm)	Drift (%)	Base Shear (KN)
Ground level	0	0	0	2404.252
First Floor	2.75	4.646	0.169	
Second Floor	5.5	9.049	0.160	
PGA = 0.75g				
Storey Level	Storey height (m)	Displacement (mm)	Drift (%)	Base Shear (KN)
Ground level	0	0	0	3005.545
First Floor	2.75	5.808	0.211	
Second Floor	5.5	11.312	0.200	
PGA = 0.9g				
Storey Level	Storey height (m)	Displacement (mm)	Drift (%)	Base Shear (KN)
Ground level	0	0	0	3606.378
First Floor	2.75	6.969	0.253	
Second Floor	5.5	13.573	0.240	
PGA = 1.0g				
Storey Level	Storey height (m)	Displacement (mm)	Drift (%)	Base Shear (KN)
Ground level	0	0	0	4007.852
First Floor	2.75	7.745	0.282	
Second Floor	5.5	15.084	0.267	

Table 4-6: Response of SCEM Building (Kobe)

Kobe Earthquake (SCEM), PGA = 0.2g				
Storey Level	Storey height (m)	Displacement (mm)	Drift (%)	Base Shear (KN)
Ground level	0	0	0	911.454
First Floor	2.75	1.645	0.060	
Second Floor	5.50	3.616	0.072	
PGA = 0.3g				
Storey Level	Storey height (m)	Displacement (mm)	Drift (%)	Base Shear (KN)
Ground level	0	0	0	1367.181
First Floor	2.75	2.468	0.090	
Second Floor	5.5	5.424	0.107	
PGA = 0.45g				
Storey Level	Storey height (m)	Displacement (mm)	Drift (%)	Base Shear (KN)
Ground level	0	0	0	2050.611
First Floor	2.75	3.702	0.135	
Second Floor	5.5	8.135	0.161	
PGA = 0.6g				
Storey Level	Storey height (m)	Displacement (mm)	Drift (%)	Base Shear (KN)
Ground level	0	0	0	2734.201
First Floor	2.75	4.936	0.179	
Second Floor	5.5	10.846	0.215	
PGA = 0.75g				
Storey Level	Storey height (m)	Displacement (mm)	Drift (%)	Base Shear (KN)
Ground level	0	0	0	3417.791
First Floor	2.75	6.170	0.224	
Second Floor	5.5	13.558	0.269	
PGA = 0.9g				
Storey Level	Storey height (m)	Displacement (mm)	Drift (%)	Base Shear (KN)
Ground level	0	0	0	4101.382
First Floor	2.75	7.403	0.269	
Second Floor	5.5	16.270	0.322	
PGA = 1.0g				
Storey Level	Storey height (m)	Displacement (mm)	Drift (%)	Base Shear (KN)
Ground level	0	0	0	4557.108
First Floor	2.75	8.226	0.299	
Second Floor	5.5	18.078	0.358	

Table 4-7: Response of SMUD Building (Gorkha)

Gorkha Earthquake (SMUD), PGA = 0.2g				
Storey Level	Storey height (m)	Displacement (mm)	Drift (%)	Base Shear (KN)
Ground level	0	0	0	670.372
First Floor	2.75	2.045	0.074	
Second Floor	5.5	2.893	0.031	
PGA = 0.3g				
Storey Level	Storey height (m)	Displacement (mm)	Drift (%)	Base Shear (KN)
Ground level	0	0	0	1005.557
First Floor	2.75	3.068	0.112	
Second Floor	5.5	4.340	0.046	
PGA = 0.45g				
Storey Level	Storey height (m)	Displacement (mm)	Drift (%)	Base Shear (KN)
Ground level	0	0	0	1508.336
First Floor	2.75	4.602	0.167	
Second Floor	5.5	6.510	0.069	
PGA = 0.6g				
Storey Level	Storey height (m)	Displacement (mm)	Drift (%)	Base Shear (KN)
Ground level	0	0	0	2011.115
First Floor	2.75	6.136	0.223	
Second Floor	5.5	8.680	0.092	
PGA = 0.75g				
Storey Level	Storey height (m)	Displacement (mm)	Drift (%)	Base Shear (KN)
Ground level	0	0	0	2513.894
First Floor	2.75	7.670	0.279	
Second Floor	5.5	10.850	0.116	
PGA = 0.9g				
Storey Level	Storey height (m)	Displacement (mm)	Drift (%)	Base Shear (KN)
Ground level	0	0	0	3016.672
First Floor	2.75	9.204	0.335	
Second Floor	5.5	13.019	0.139	
PGA = 1.0g				
Storey Level	Storey height (m)	Displacement (mm)	Drift (%)	Base Shear (KN)
Ground level	0	0	0	3351.858
First Floor	2.75	10.227	0.372	
Second Floor	5.5	14.466	0.154	

Table 4-8: Response of SMUD Building (Imp Valley)

Imp Valley Earthquake (SMUD), PGA = 0.2g				
Storey Level	Storey height (m)	Displacement (mm)	Drift (%)	Base Shear (KN)
Ground level	0	0	0	1243.441
First Floor	2.75	3.362	0.122	
Second Floor	5.50	5.223	0.068	
PGA = 0.3g				
Storey Level	Storey height (m)	Displacement (mm)	Drift (%)	Base Shear (KN)
Ground level	0	0	0	1866.942
First Floor	2.75	5.048	0.184	
Second Floor	5.5	7.841	0.102	
PGA = 0.45g				
Storey Level	Storey height (m)	Displacement (mm)	Drift (%)	Base Shear (KN)
Ground level	0	0	0	2800.414
First Floor	2.75	7.572	0.275	
Second Floor	5.5	11.762	0.152	
PGA = 0.6g				
Storey Level	Storey height (m)	Displacement (mm)	Drift (%)	Base Shear (KN)
Ground level	0	0	0	3733.885
First Floor	2.75	10.096	0.367	
Second Floor	5.5	15.683	0.203	
PGA = 0.75g				
Storey Level	Storey height (m)	Displacement (mm)	Drift (%)	Base Shear (KN)
Ground level	0	0	0	4667.712
First Floor	2.75	12.621	0.459	
Second Floor	5.5	19.605	0.254	
PGA = 0.9g				
Storey Level	Storey height (m)	Displacement (mm)	Drift (%)	Base Shear (KN)
Ground level	0	0	0	5600.827
First Floor	2.75	15.144	0.551	
Second Floor	5.5	23.524	0.305	
PGA = 1.0g				
Storey Level	Storey height (m)	Displacement (mm)	Drift (%)	Base Shear (KN)
Ground level	0	0	0	6224.329
First Floor	2.75	16.830	0.612	
Second Floor	5.5	26.143	0.339	

Table 4-9: Response of SMUD Building (Kobe)

Kobe Earthquake (SMUD), PGA = 0.2g				
Storey Level	Storey height (m)	Displacement (mm)	Drift (%)	Base Shear (KN)
Ground level	0	0	0	1325.669
First Floor	2.75	3.848	0.140	
Second Floor	5.50	6.010	0.079	
PGA = 0.3g				
Storey Level	Storey height (m)	Displacement (mm)	Drift (%)	Base Shear (KN)
Ground level	0	0	0	1988.504
First Floor	2.75	5.772	0.210	
Second Floor	5.5	9.016	0.118	
PGA = 0.45g				
Storey Level	Storey height (m)	Displacement (mm)	Drift (%)	Base Shear (KN)
Ground level	0	0	0	2982.523
First Floor	2.75	8.657	0.315	
Second Floor	5.5	13.522	0.177	
PGA = 0.6g				
Storey Level	Storey height (m)	Displacement (mm)	Drift (%)	Base Shear (KN)
Ground level	0	0	0	3976.775
First Floor	2.75	11.543	0.420	
Second Floor	5.5	18.030	0.236	
PGA = 0.75g				
Storey Level	Storey height (m)	Displacement (mm)	Drift (%)	Base Shear (KN)
Ground level	0	0	0	4971.027
First Floor	2.75	14.429	0.525	
Second Floor	5.5	22.538	0.295	
PGA = 0.9g				
Storey Level	Storey height (m)	Displacement (mm)	Drift (%)	Base Shear (KN)
Ground level	0	0	0	5965.279
First Floor	2.75	17.315	0.630	
Second Floor	5.5	27.045	0.354	
PGA = 1.0g				
Storey Level	Storey height (m)	Displacement (mm)	Drift (%)	Base Shear (KN)
Ground level	0	0	0	6628.114
First Floor	2.75	19.239	0.700	
Second Floor	5.5	30.051	0.393	

Table 4-10: Response of CSEB Building (Gorkha)

Gorkha Earthquake (CSEB), PGA = 0.2g				
Storey Level	Storey height (m)	Displacement (mm)	Drift (%)	Base Shear (KN)
Ground level	0	0	0	356.246
First Floor	2.75	1.553	0.056	
Second Floor	5.5	1.981	0.016	
PGA = 0.3g				
Storey Level	Storey height (m)	Displacement (mm)	Drift (%)	Base Shear (KN)
Ground level	0	0	0	534.369
First Floor	2.75	2.329	0.085	
Second Floor	5.5	2.971	0.023	
PGA = 0.45g				
Storey Level	Storey height (m)	Displacement (mm)	Drift (%)	Base Shear (KN)
Ground level	0	0	0	801.554
First Floor	2.75	3.493	0.127	
Second Floor	5.5	4.457	0.035	
PGA = 0.6g				
Storey Level	Storey height (m)	Displacement (mm)	Drift (%)	Base Shear (KN)
Ground level	0	0	0	1068.739
First Floor	2.75	4.658	0.169	
Second Floor	5.5	5.943	0.047	
PGA = 0.75g				
Storey Level	Storey height (m)	Displacement (mm)	Drift (%)	Base Shear (KN)
Ground level	0	0	0	1335.924
First Floor	2.75	5.822	0.212	
Second Floor	5.5	7.428	0.058	
PGA = 0.9g				
Storey Level	Storey height (m)	Displacement (mm)	Drift (%)	Base Shear (KN)
Ground level	0	0	0	1603.108
First Floor	2.75	6.987	0.254	
Second Floor	5.5	8.914	0.070	
PGA = 1.0g				
Storey Level	Storey height (m)	Displacement (mm)	Drift (%)	Base Shear (KN)
Ground level	0	0	0	1781.232
First Floor	2.75	7.763	0.282	
Second Floor	5.5	9.904	0.078	

Table 4-11: Response of CSEB Building (Imp Valley)

Imp Valley Earthquake (CSEB), PGA = 0.2g				
Storey Level	Storey height (m)	Displacement (mm)	Drift (%)	Base Shear (KN)
Ground level	0	0	0	660.867
First Floor	2.75	2.627	0.096	
Second Floor	5.50	3.745	0.041	
PGA = 0.3g				
Storey Level	Storey height (m)	Displacement (mm)	Drift (%)	Base Shear (KN)
Ground level	0	0	0	992.248
First Floor	2.75	3.945	0.143	
Second Floor	5.5	5.623	0.061	
PGA = 0.45g				
Storey Level	Storey height (m)	Displacement (mm)	Drift (%)	Base Shear (KN)
Ground level	0	0	0	1488.372
First Floor	2.75	5.917	0.215	
Second Floor	5.5	8.434	0.092	
PGA = 0.6g				
Storey Level	Storey height (m)	Displacement (mm)	Drift (%)	Base Shear (KN)
Ground level	0	0	0	1984.496
First Floor	2.75	7.889	0.287	
Second Floor	5.5	11.246	0.122	
PGA = 0.75g				
Storey Level	Storey height (m)	Displacement (mm)	Drift (%)	Base Shear (KN)
Ground level	0	0	0	2480.809
First Floor	2.75	9.862	0.359	
Second Floor	5.5	14.058	0.153	
PGA = 0.9g				
Storey Level	Storey height (m)	Displacement (mm)	Drift (%)	Base Shear (KN)
Ground level	0	0	0	2976.744
First Floor	2.75	11.834	0.430	
Second Floor	5.5	16.869	0.183	
PGA = 1.0g				
Storey Level	Storey height (m)	Displacement (mm)	Drift (%)	Base Shear (KN)
Ground level	0	0	0	3308.124
First Floor	2.75	13.151	0.478	
Second Floor	5.5	18.747	0.203	

Table 4-12: Response of CSEB Building (Kobe)

Kobe Earthquake (CSEB), PGA = 0.2g				
Storey Level	Storey height (m)	Displacement (mm)	Drift (%)	Base Shear (KN)
Ground level	0	0	0	817.829
First Floor	2.75	4.016	0.146	
Second Floor	5.50	5.405	0.050	
PGA = 0.3g				
Storey Level	Storey height (m)	Displacement (mm)	Drift (%)	Base Shear (KN)
Ground level	0	0	0	1226.743
First Floor	2.75	6.024	0.219	
Second Floor	5.5	8.107	0.076	
PGA = 0.45g				
Storey Level	Storey height (m)	Displacement (mm)	Drift (%)	Base Shear (KN)
Ground level	0	0	0	1839.971
First Floor	2.75	9.035	0.329	
Second Floor	5.5	12.159	0.114	
PGA = 0.6g				
Storey Level	Storey height (m)	Displacement (mm)	Drift (%)	Base Shear (KN)
Ground level	0	0	0	2453.342
First Floor	2.75	12.047	0.438	
Second Floor	5.5	16.213	0.151	
PGA = 0.75g				
Storey Level	Storey height (m)	Displacement (mm)	Drift (%)	Base Shear (KN)
Ground level	0	0	0	3066.713
First Floor	2.75	15.059	0.548	
Second Floor	5.5	20.266	0.189	
PGA = 0.9g				
Storey Level	Storey height (m)	Displacement (mm)	Drift (%)	Base Shear (KN)
Ground level	0	0	0	3680.085
First Floor	2.75	18.071	0.657	
Second Floor	5.5	24.320	0.227	
PGA = 1.0g				
Storey Level	Storey height (m)	Displacement (mm)	Drift (%)	Base Shear (KN)
Ground level	0	0	0	4088.999
First Floor	2.75	20.079	0.730	
Second Floor	5.5	27.022	0.252	

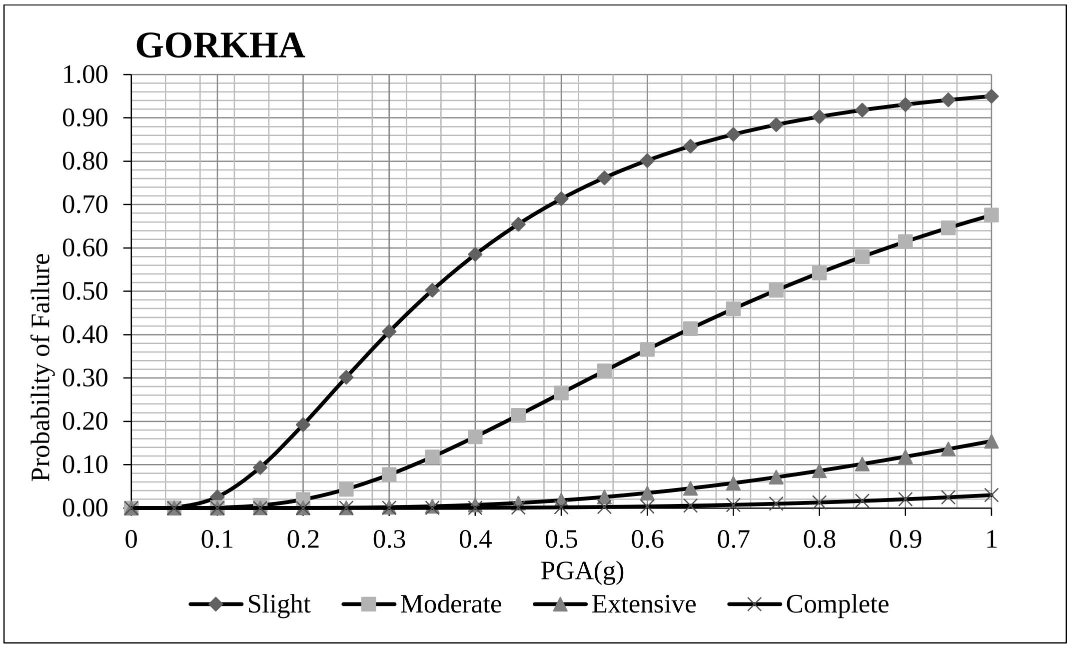

Figure 4-3: Fragility Curve for BCEM typology for various damage state for Gorkha Earthquake

Table 4-13: Calculation of Probability of failure for BCEM (Gorkha Earthquake)

BCEM									
PGA (g)	**Top displacement (mm)**					**Probability of failure at damage state (pf)**			
	Demand (mm) Sd	**Capacity Displacement mm (Sc)**							
	Gorkha	**Slight**	**Moderate**	**Extensive**	**Complete**	**Slight**	**Moderate**	**Extensive**	**Complete**
0.00	0.000	0.000	0.000	0.000	0.000	0.000	0.000	0.000	0.000
0.05	0.308	2.844	6.096	22.326	40.589	0.001	0.000	0.000	0.000
0.10	0.616	2.844	6.096	22.326	40.589	0.015	0.000	0.000	0.000
0.15	0.923	2.844	6.096	22.326	40.589	0.062	0.003	0.000	0.000
0.20	1.231	2.844	6.096	22.326	40.589	0.138	0.011	0.000	0.000
0.25	1.539	2.844	6.096	22.326	40.589	0.229	0.027	0.000	0.000
0.30	1.847	2.844	6.096	22.326	40.589	0.324	0.050	0.001	0.000
0.35	2.154	2.844	6.096	22.326	40.589	0.414	0.080	0.002	0.000
0.40	2.462	2.844	6.096	22.326	40.589	0.497	0.115	0.004	0.000
0.45	2.770	2.844	6.096	22.326	40.589	0.570	0.155	0.006	0.000
0.50	3.078	2.844	6.096	22.326	40.589	0.633	0.198	0.010	0.001
0.55	3.386	2.844	6.096	22.326	40.589	0.688	0.242	0.015	0.001
0.60	3.693	2.844	6.096	22.326	40.589	0.734	0.286	0.021	0.002
0.65	4.001	2.844	6.096	22.326	40.589	0.774	0.330	0.028	0.003
0.70	4.309	2.844	6.096	22.326	40.589	0.807	0.373	0.036	0.004
0.75	4.617	2.844	6.096	22.326	40.589	0.835	0.414	0.046	0.005
0.80	4.924	2.844	6.096	22.326	40.589	0.859	0.454	0.056	0.007
0.85	5.232	2.844	6.096	22.326	40.589	0.879	0.492	0.068	0.009
0.90	5.540	2.844	6.096	22.326	40.589	0.896	0.527	0.080	0.012
0.95	5.848	2.844	6.096	22.326	40.589	0.910	0.561	0.093	0.014
1	6.156	2.844	6.096	22.326	40.589	0.923	0.592	0.107	0.018

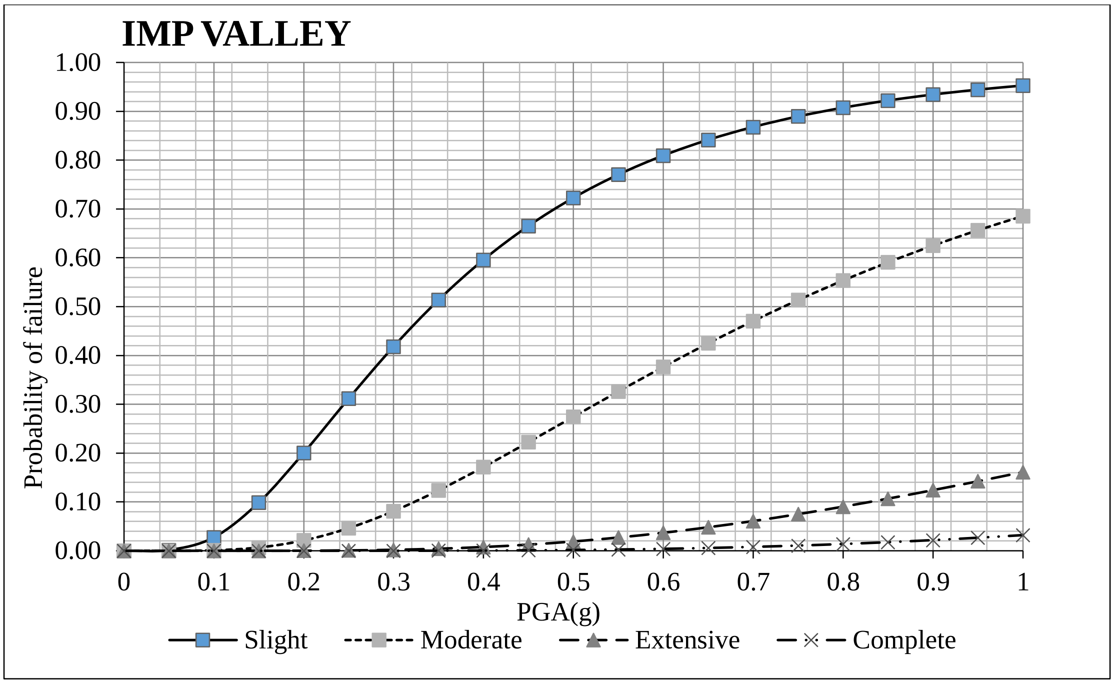

Figure 4-4: Fragility curve for BCEM for various damage state for Imperial Valley Earthquake

Table 4-14: Calculation of Probability of failure for BCEM (Imp Valley Earthquake)

PGA (g)	Top displacement (mm)					Probability of failure at damage state (pf)			
	Demand (mm) Sd	Capacity Displacement mm (Sc)							
	Imp Valley	Slight	Moderate	Extensive	Complete	Slight	Moderate	Extensive	Complete
0.00	0.000	0.000	0.000	0.000	0.000	0.000	0.000	0.000	0.000
0.05	0.405	2.844	6.096	22.326	40.589	0.001	0.000	0.000	0.000
0.1	0.811	2.844	6.096	22.326	40.589	0.027	0.001	0.000	0.000
0.15	1.216	2.844	6.096	22.326	40.589	0.099	0.007	0.000	0.000
0.2	1.621	2.844	6.096	22.326	40.589	0.200	0.021	0.000	0.000
0.25	2.026	2.844	6.096	22.326	40.589	0.312	0.046	0.001	0.000
0.3	2.432	2.844	6.096	22.326	40.589	0.418	0.081	0.002	0.000
0.35	2.837	2.844	6.096	22.326	40.589	0.514	0.124	0.004	0.000
0.4	3.242	2.844	6.096	22.326	40.589	0.596	0.172	0.008	0.001
0.45	3.648	2.844	6.096	22.326	40.589	0.665	0.223	0.013	0.001
0.5	4.053	2.844	6.096	22.326	40.589	0.723	0.275	0.019	0.002
0.55	4.458	2.844	6.096	22.326	40.589	0.771	0.326	0.027	0.003
0.6	4.864	2.844	6.096	22.326	40.589	0.810	0.377	0.037	0.004
0.65	5.269	2.844	6.096	22.326	40.589	0.842	0.425	0.048	0.006
0.7	5.674	2.844	6.096	22.326	40.589	0.868	0.471	0.061	0.008
0.75	6.079	2.844	6.096	22.326	40.589	0.890	0.514	0.075	0.011
0.8	6.485	2.844	6.096	22.326	40.589	0.908	0.554	0.090	0.014
0.85	6.890	2.844	6.096	22.326	40.589	0.922	0.591	0.107	0.017
0.9	7.295	2.844	6.096	22.326	40.589	0.935	0.625	0.124	0.022
0.95	7.701	2.844	6.096	22.326	40.589	0.945	0.657	0.142	0.026
1	8.106	2.844	6.096	22.326	40.589	0.953	0.686	0.161	0.032

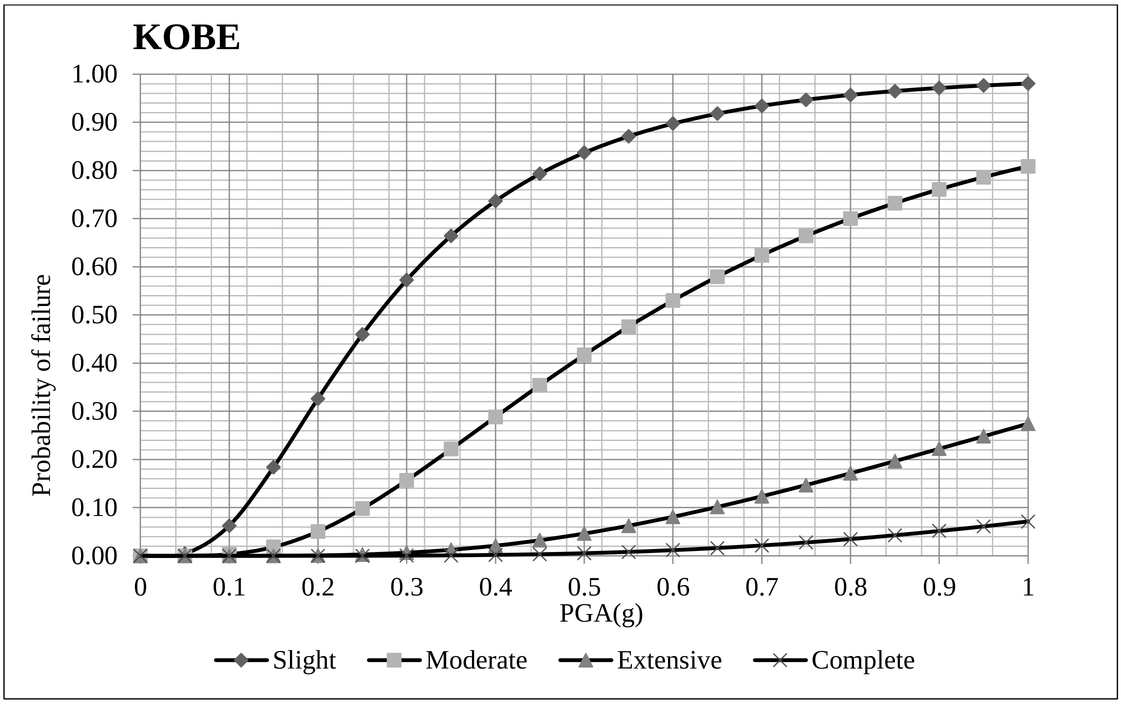

Figure 4-5: Fragility curve for BCEM for various damage state for Kobe Earthquake

Table 4-15: Calculation of Probability of failure for BCEM (Kobe Earthquake)

PGA (g)	Top displacement (mm)					Probability of failure at damage state (pf)			
	Demand (mm) Sd	Capacity Displacement mm (Sc)							
	Kobe	Slight	Moderate	Extensive	Complete	Slight	Moderate	Extensive	Complete
0.00	0.000	0.000	0.000	0.000	0.000	0.000	0.000	0.000	0.000
0.05	0.652	2.844	6.096	22.326	40.589	0.004	0.000	0.000	0.000
0.10	1.305	2.844	6.096	22.326	40.589	0.063	0.003	0.000	0.000
0.15	1.957	2.844	6.096	22.326	40.589	0.184	0.018	0.000	0.000
0.20	2.609	2.844	6.096	22.326	40.589	0.326	0.050	0.001	0.000
0.25	3.262	2.844	6.096	22.326	40.589	0.459	0.098	0.003	0.000
0.30	3.914	2.844	6.096	22.326	40.589	0.573	0.157	0.007	0.000
0.35	4.566	2.844	6.096	22.326	40.589	0.664	0.222	0.013	0.001
0.40	5.219	2.844	6.096	22.326	40.589	0.736	0.288	0.021	0.002
0.45	5.871	2.844	6.096	22.326	40.589	0.793	0.354	0.032	0.003
0.50	6.524	2.844	6.096	22.326	40.589	0.837	0.417	0.046	0.005
0.55	7.176	2.844	6.096	22.326	40.589	0.871	0.476	0.062	0.008
0.60	7.828	2.844	6.096	22.326	40.589	0.897	0.530	0.081	0.012
0.65	8.481	2.844	6.096	22.326	40.589	0.918	0.579	0.101	0.016
0.70	9.133	2.844	6.096	22.326	40.589	0.934	0.624	0.124	0.022
0.75	9.785	2.844	6.096	22.326	40.589	0.947	0.664	0.147	0.028
0.80	10.438	2.844	6.096	22.326	40.589	0.957	0.700	0.171	0.035
0.85	11.090	2.844	6.096	22.326	40.589	0.965	0.732	0.197	0.043
0.90	11.742	2.844	6.096	22.326	40.589	0.971	0.761	0.222	0.051
0.95	12.395	2.844	6.096	22.326	40.589	0.976	0.786	0.248	0.061
1.00	13.047	2.844	6.096	22.326	40.589	0.981	0.809	0.274	0.071

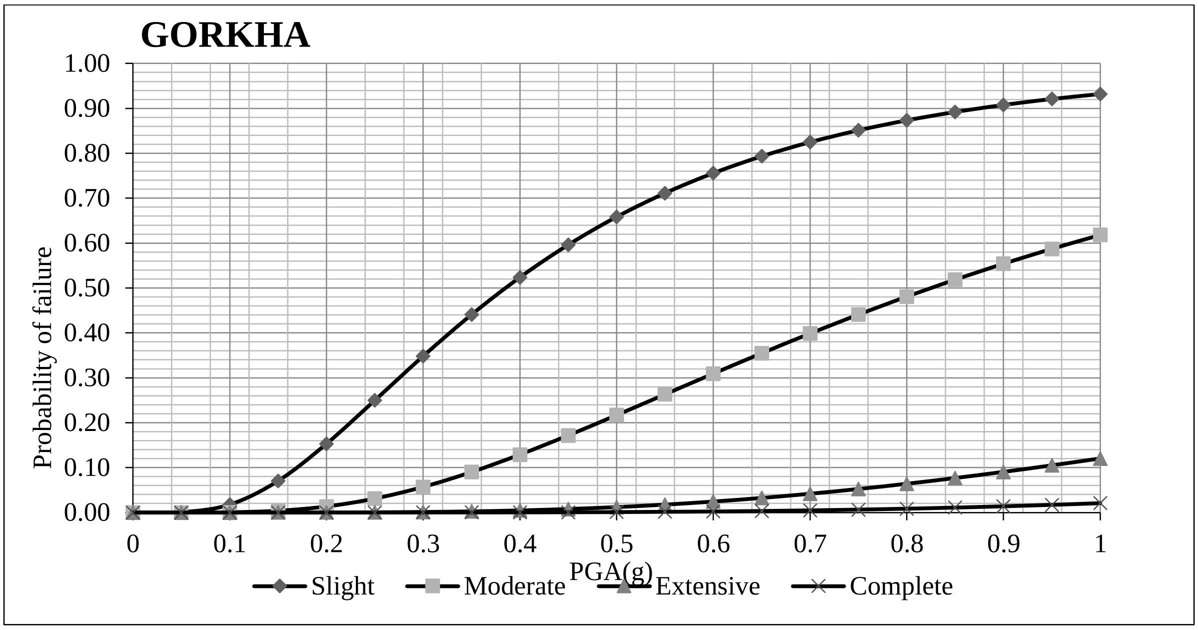

Figure 4-6: Fragility curve for SCEM for various damage state for Gorkha Earthquake

Table 4-16: Calculation of Probability of failure for SCEM (Gorkha Earthquake)

PGA (g)	Top displacement (mm)					Probability of failure at damage state (pf)			
	Demand (mm) Sd	Capacity Displacement mm (Sc)							
	Gorkha	Slight	Moderate	Extensive	Complete	Slight	Moderate	Extensive	Complete
0.00	0.000	0.000	0.000	0.000	0.000	0.000	0.000	0.000	0.000
0.05	0.410	2.844	6.096	22.326	40.589	0.001	0.000	0.000	0.000
0.10	0.820	2.844	6.096	22.326	40.589	0.018	0.000	0.000	0.000
0.15	1.230	2.844	6.096	22.326	40.589	0.070	0.004	0.000	0.000
0.20	1.640	2.844	6.096	22.326	40.589	0.153	0.013	0.000	0.000
0.25	2.051	2.844	6.096	22.326	40.589	0.250	0.031	0.000	0.000
0.30	2.461	2.844	6.096	22.326	40.589	0.348	0.057	0.001	0.000
0.35	2.871	2.844	6.096	22.326	40.589	0.441	0.090	0.002	0.000
0.40	3.281	2.844	6.096	22.326	40.589	0.524	0.129	0.005	0.000
0.45	3.691	2.844	6.096	22.326	40.589	0.596	0.172	0.008	0.001
0.50	4.101	2.844	6.096	22.326	40.589	0.658	0.217	0.012	0.001
0.55	4.511	2.844	6.096	22.326	40.589	0.711	0.263	0.018	0.001
0.60	4.921	2.844	6.096	22.326	40.589	0.756	0.309	0.024	0.002
0.65	5.331	2.844	6.096	22.326	40.589	0.793	0.355	0.032	0.003
0.70	5.741	2.844	6.096	22.326	40.589	0.825	0.399	0.042	0.005
0.75	6.152	2.844	6.096	22.326	40.589	0.851	0.441	0.052	0.006
0.80	6.562	2.844	6.096	22.326	40.589	0.873	0.481	0.064	0.008
0.85	6.972	2.844	6.096	22.326	40.589	0.892	0.518	0.077	0.011
0.90	7.382	2.844	6.096	22.326	40.589	0.908	0.554	0.090	0.014
0.95	7.792	2.844	6.096	22.326	40.589	0.921	0.587	0.105	0.017
1	8.202	2.844	6.096	22.326	40.589	0.932	0.618	0.120	0.021

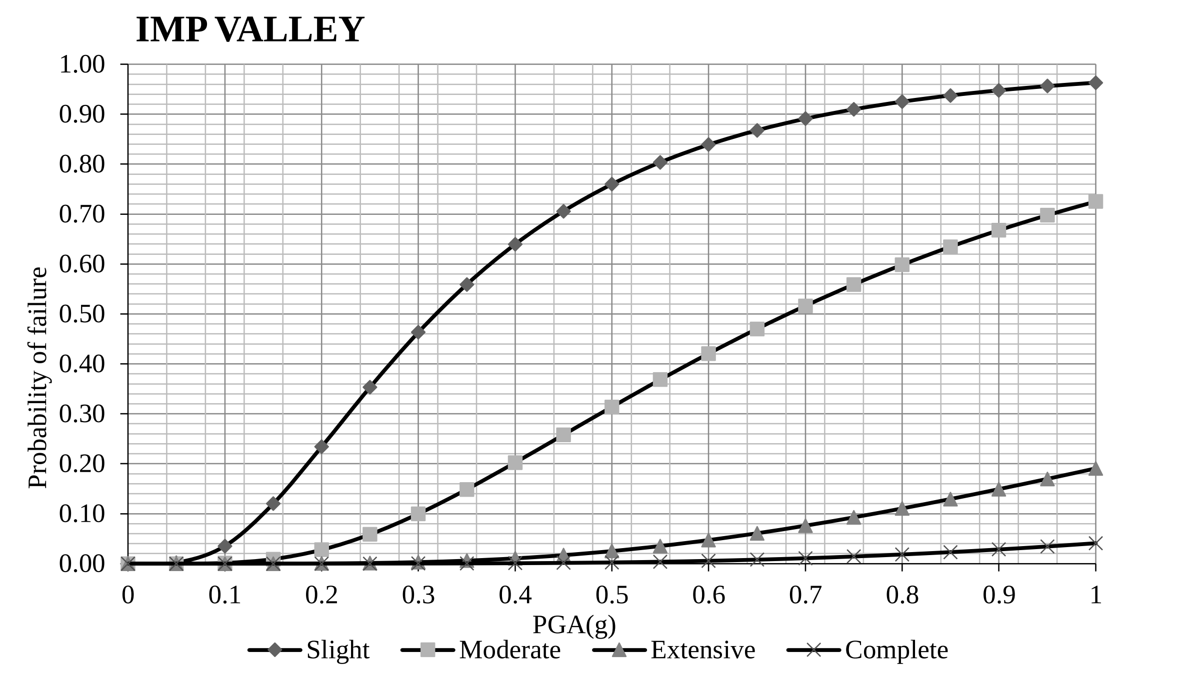

Figure 4-7: Fragility curve for SCEM for various damage state for Imperial Valley Earthquake

Table 4-17: Calculation of Probability of failure for SCEM (Imp Valley Earthquake)

PGA (g)	Top displacement (mm)					Probability of failure at damage state (pf)			
	Demand (mm) Sd	Capacity Displacement mm (Sc)							
	Imp Valley	Slight	Moderate	Extensive	Complete	Slight	Moderate	Extensive	Complete
0.00	0.000	0.000	0.000	0.000	0.000	0.000	0.000	0.000	0.000
0.05	0.754	2.844	6.096	22.326	40.589	0.002	0.000	0.000	0.000
0.1	1.508	2.844	6.096	22.326	40.589	0.035	0.001	0.000	0.000
0.15	2.263	2.844	6.096	22.326	40.589	0.120	0.009	0.000	0.000
0.2	3.017	2.844	6.096	22.326	40.589	0.234	0.028	0.000	0.000
0.25	3.771	2.844	6.096	22.326	40.589	0.353	0.058	0.001	0.000
0.3	4.525	2.844	6.096	22.326	40.589	0.463	0.100	0.003	0.000
0.35	5.279	2.844	6.096	22.326	40.589	0.559	0.149	0.006	0.000
0.4	6.034	2.844	6.096	22.326	40.589	0.639	0.202	0.011	0.001
0.45	6.788	2.844	6.096	22.326	40.589	0.706	0.258	0.017	0.001
0.5	7.542	2.844	6.096	22.326	40.589	0.760	0.314	0.025	0.002
0.55	8.296	2.844	6.096	22.326	40.589	0.804	0.368	0.035	0.004
0.6	9.050	2.844	6.096	22.326	40.589	0.839	0.421	0.047	0.006
0.65	9.805	2.844	6.096	22.326	40.589	0.868	0.470	0.061	0.008
0.7	10.559	2.844	6.096	22.326	40.589	0.891	0.516	0.076	0.011
0.75	11.313	2.844	6.096	22.326	40.589	0.910	0.559	0.093	0.014
0.8	12.067	2.844	6.096	22.326	40.589	0.925	0.598	0.110	0.018
0.85	12.821	2.844	6.096	22.326	40.589	0.938	0.635	0.129	0.023
0.9	13.576	2.844	6.096	22.326	40.589	0.948	0.668	0.149	0.028
0.95	14.330	2.844	6.096	22.326	40.589	0.956	0.698	0.170	0.034
1	15.084	2.844	6.096	22.326	40.589	0.963	0.725	0.191	0.041

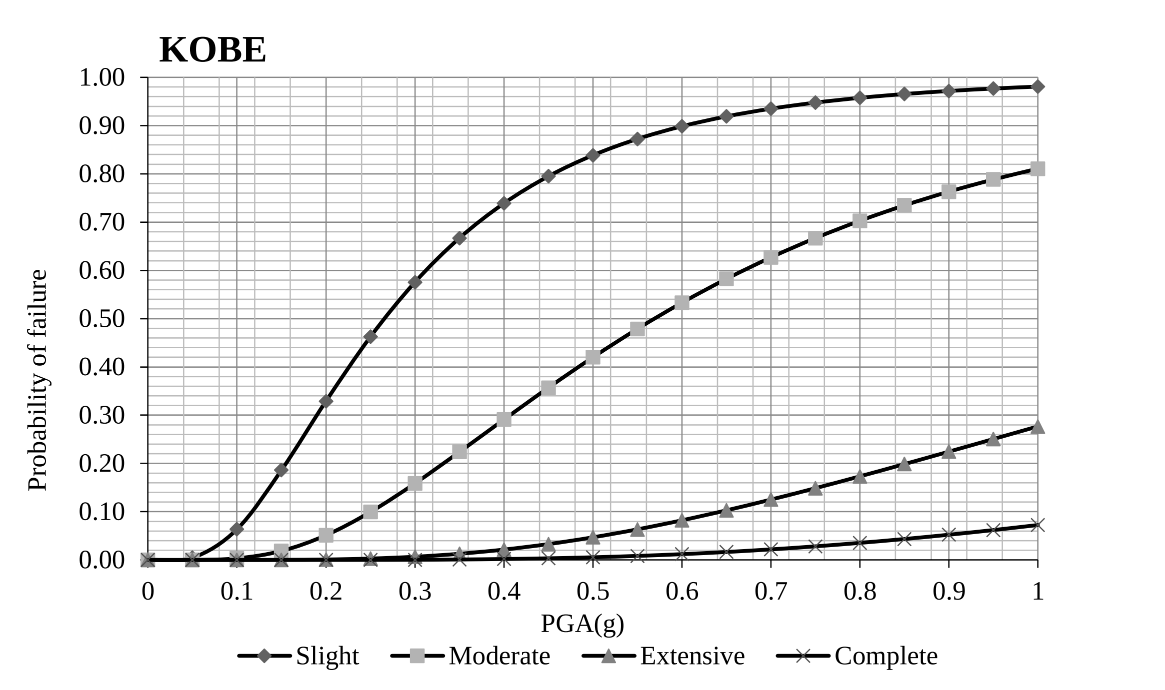

Figure 4-8: Fragility curve for SCEM for various damage state for Kobe Earthquake

Table 4-18: Calculation of Probability of failure for SCEM (Kobe Earthquake)

PGA (g)	Top displacement (mm)					Probability of failure at damage state (pf)			
	Demand (mm) Sd	Capacity Displacement mm (Sc)							
	Kobe	Slight	Moderate	Extensive	Complete	Slight	Moderate	Extensive	Complete
0.00	0.000	0.000	0.000	0.000	0.000	0.000	0.000	0.000	0.000
0.05	0.904	2.844	6.096	22.326	40.589	0.005	0.000	0.000	0.000
0.10	1.808	2.844	6.096	22.326	40.589	0.063	0.003	0.000	0.000
0.15	2.712	2.844	6.096	22.326	40.589	0.186	0.019	0.000	0.000
0.20	3.616	2.844	6.096	22.326	40.589	0.329	0.051	0.001	0.000
0.25	4.520	2.844	6.096	22.326	40.589	0.462	0.099	0.003	0.000
0.30	5.423	2.844	6.096	22.326	40.589	0.576	0.159	0.007	0.000
0.35	6.327	2.844	6.096	22.326	40.589	0.667	0.224	0.013	0.001
0.40	7.231	2.844	6.096	22.326	40.589	0.739	0.291	0.021	0.002
0.45	8.135	2.844	6.096	22.326	40.589	0.795	0.357	0.033	0.003
0.50	9.039	2.844	6.096	22.326	40.589	0.839	0.420	0.047	0.006
0.55	9.943	2.844	6.096	22.326	40.589	0.872	0.479	0.063	0.008
0.60	10.847	2.844	6.096	22.326	40.589	0.899	0.533	0.082	0.012
0.65	11.751	2.844	6.096	22.326	40.589	0.919	0.582	0.103	0.017
0.70	12.655	2.844	6.096	22.326	40.589	0.935	0.627	0.125	0.022
0.75	13.559	2.844	6.096	22.326	40.589	0.948	0.667	0.149	0.028
0.80	14.462	2.844	6.096	22.326	40.589	0.958	0.703	0.173	0.035
0.85	15.366	2.844	6.096	22.326	40.589	0.965	0.735	0.199	0.043
0.90	16.270	2.844	6.096	22.326	40.589	0.972	0.763	0.224	0.052
0.95	17.174	2.844	6.096	22.326	40.589	0.977	0.788	0.251	0.062
1.00	18.078	2.844	6.096	22.326	40.589	0.981	0.811	0.277	0.072

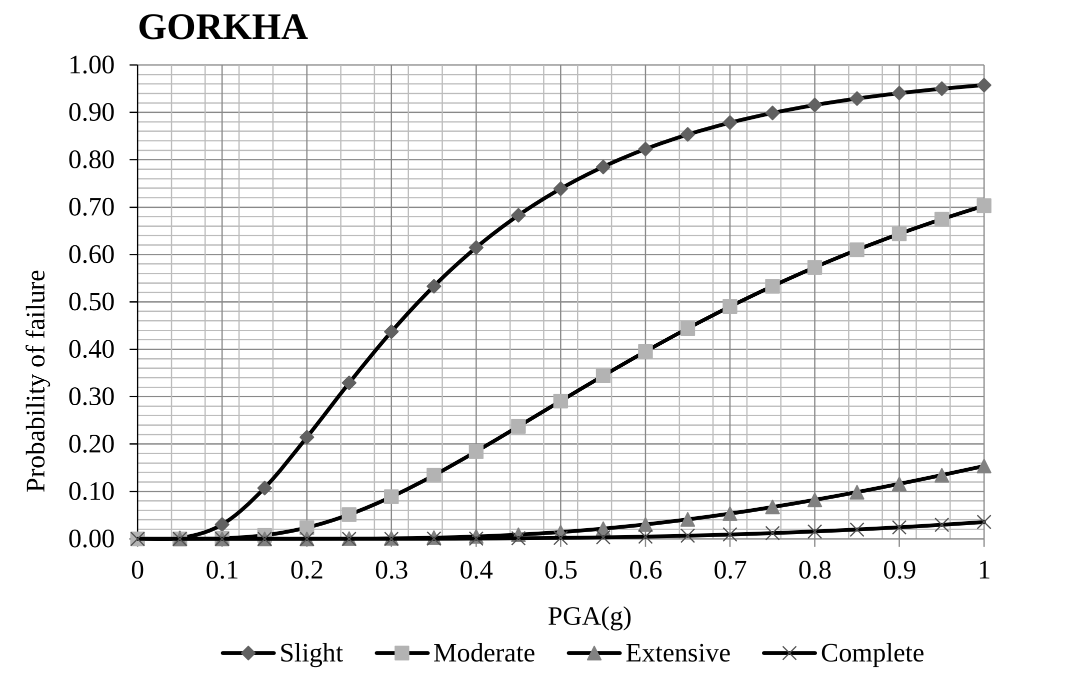

Figure 4-9: Fragility curve for SMUD for various damage state for Gorkha Earthquake

Table 4-19: Calculation of Probability of failure for SMUD (Gorkha Earthquake)

PGA (g)	Top displacement (mm)					Probability of failure at damage state (pf)			
	Demand (mm) Sd	Capacity Displacement mm (Sc)							
	Gorkha	Slight	Moderate	Extensive	Complete	Slight	Moderate	Extensive	Complete
0.00	0.000	0.000	0.000	0.000	0.000	0.000	0.000	0.000	0.000
0.05	0.723	2.844	6.096	22.326	40.589	0.002	0.000	0.000	0.000
0.10	1.447	2.844	6.096	22.326	40.589	0.030	0.001	0.000	0.000
0.15	2.170	2.844	6.096	22.326	40.589	0.107	0.008	0.000	0.000
0.20	2.893	2.844	6.096	22.326	40.589	0.214	0.024	0.000	0.000
0.25	3.617	2.844	6.096	22.326	40.589	0.329	0.051	0.001	0.000
0.30	4.340	2.844	6.096	22.326	40.589	0.437	0.089	0.002	0.000
0.35	5.063	2.844	6.096	22.326	40.589	0.533	0.134	0.005	0.000
0.40	5.786	2.844	6.096	22.326	40.589	0.615	0.184	0.009	0.001
0.45	6.510	2.844	6.096	22.326	40.589	0.683	0.237	0.014	0.001
0.50	7.233	2.844	6.096	22.326	40.589	0.739	0.291	0.021	0.002
0.55	7.956	2.844	6.096	22.326	40.589	0.785	0.344	0.030	0.003
0.60	8.680	2.844	6.096	22.326	40.589	0.823	0.395	0.041	0.005
0.65	9.403	2.844	6.096	22.326	40.589	0.853	0.444	0.053	0.007
0.70	10.126	2.844	6.096	22.326	40.589	0.878	0.490	0.067	0.009
0.75	10.850	2.844	6.096	22.326	40.589	0.899	0.533	0.082	0.012
0.80	11.573	2.844	6.096	22.326	40.589	0.915	0.573	0.099	0.016
0.85	12.296	2.844	6.096	22.326	40.589	0.929	0.610	0.116	0.020
0.90	13.019	2.844	6.096	22.326	40.589	0.940	0.644	0.134	0.024
0.95	13.743	2.844	6.096	22.326	40.589	0.950	0.675	0.154	0.030
1	14.466	2.844	6.096	22.326	40.589	0.958	0.703	0.173	0.035

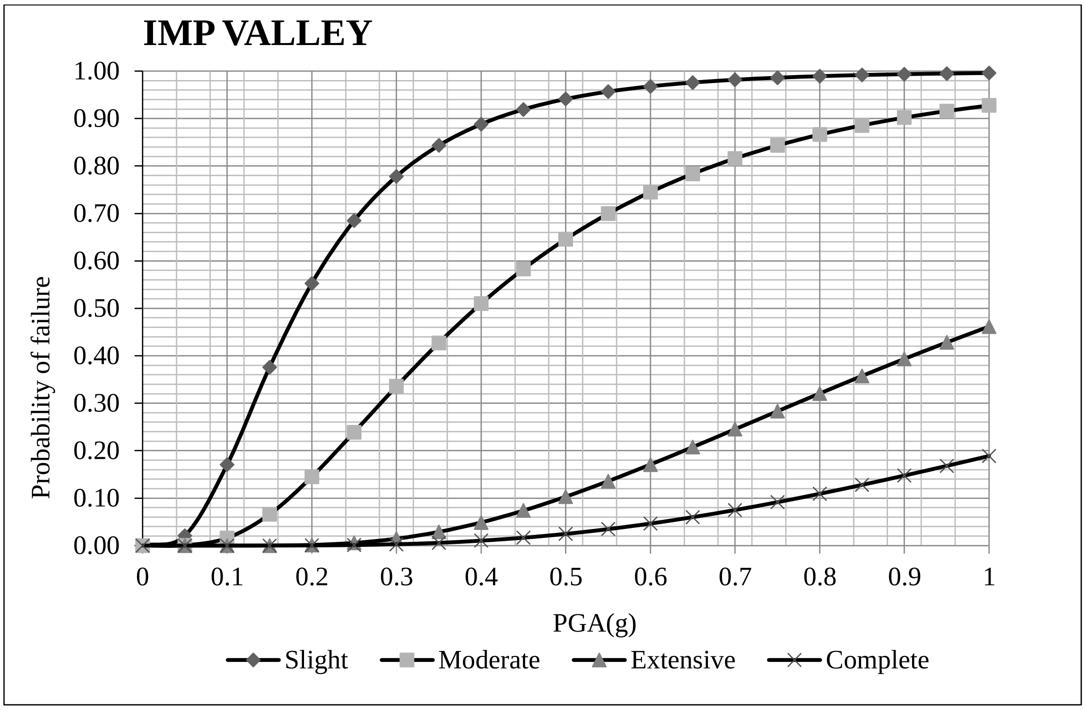

Figure 4-10: Fragility curve for SMUD for various damage state for Imperial Valley Earthquake

Table 4-20: Calculation of Probability of failure for SMUD (Imp Valley Earthquake)

PGA (g)	Top displacement (mm)					Probability of failure at damage state (pf)			
	Demand (mm) Sd	Capacity Displacement mm (Sc)							
	Imp Valley	Slight	Moderate	Extensive	Complete	Slight	Moderate	Extensive	Complete
0.00	0.000	0.000	0.000	0.000	0.000	0.000	0.000	0.000	0.000
0.05	1.305	2.844	6.096	22.326	40.589	0.021	0.001	0.000	0.000
0.1	2.612	2.844	6.096	22.326	40.589	0.171	0.016	0.000	0.000
0.15	3.919	2.844	6.096	22.326	40.589	0.376	0.066	0.001	0.000
0.2	5.226	2.844	6.096	22.326	40.589	0.553	0.145	0.006	0.000
0.25	6.533	2.844	6.096	22.326	40.589	0.685	0.239	0.015	0.001
0.3	7.840	2.844	6.096	22.326	40.589	0.778	0.336	0.029	0.003
0.35	9.148	2.844	6.096	22.326	40.589	0.843	0.427	0.049	0.006
0.4	10.455	2.844	6.096	22.326	40.589	0.888	0.480	0.074	0.010
0.45	11.762	2.844	6.096	22.326	40.589	0.919	0.583	0.103	0.017
0.5	13.069	2.844	6.096	22.326	40.589	0.941	0.646	0.136	0.025
0.55	14.376	2.844	6.096	22.326	40.589	0.957	0.699	0.171	0.035
0.6	15.683	2.844	6.096	22.326	40.589	0.968	0.745	0.208	0.046
0.65	16.990	2.844	6.096	22.326	40.589	0.976	0.783	0.245	0.060
0.7	18.298	2.844	6.096	22.326	40.589	0.982	0.816	0.283	0.075
0.75	19.605	2.844	6.096	22.326	40.589	0.986	0.843	0.321	0.091
0.8	20.912	2.844	6.096	22.326	40.589	0.989	0.866	0.358	0.109
0.85	22.219	2.844	6.096	22.326	40.589	0.992	0.886	0.393	0.128
0.9	23.526	2.844	6.096	22.326	40.589	0.993	0.902	0.428	0.148
0.95	24.833	2.844	6.096	22.326	40.589	0.995	0.916	0.462	0.168
1	26.141	2.844	6.096	22.326	40.589	0.996	0.927	0.493	0.189

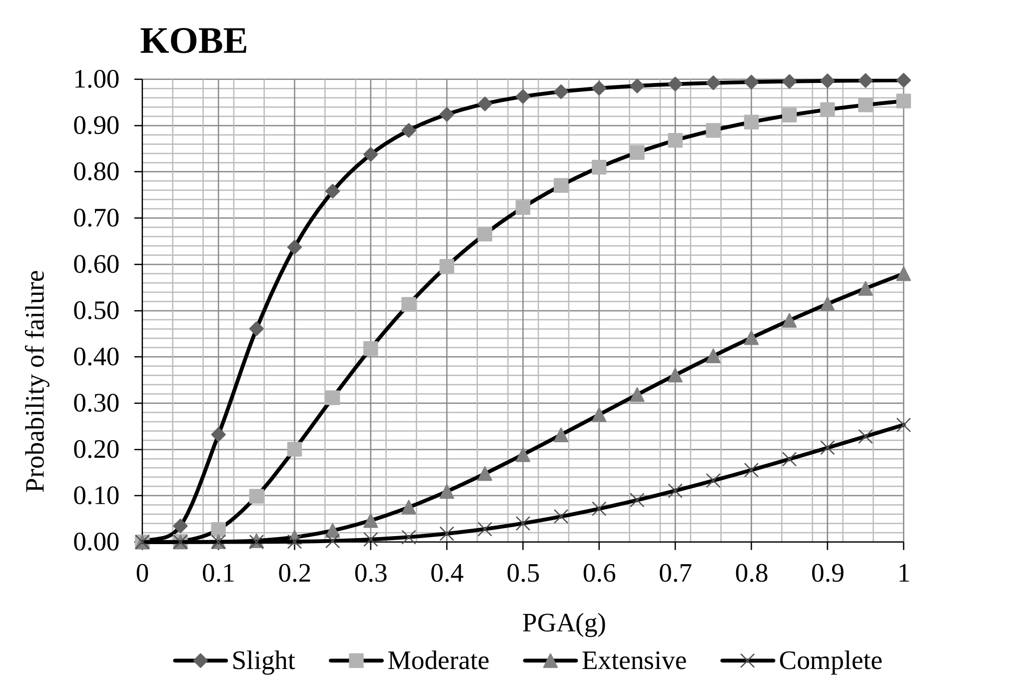

Figure 4-11: Fragility curve for SMUD for various damage state for Kobe Earthquake

Table 4-21: Calculation of Probability of failure for SMUD (Kobe Earthquake)

PGA (g)	Top displacement (mm)					Probability of failure at damage state (pf)			
	Demand (mm) Sd	Capacity Displacement mm (Sc)							
	Kobe	Slight	Moderate	Extensive	Complete	Slight	Moderate	Extensive	Complete
0.00	0.000	0.000	0.000	0.000	0.000	0.000	0.000	0.000	0.000
0.05	1.503	2.844	6.096	22.326	40.589	0.035	0.001	0.000	0.000
0.10	3.005	2.844	6.096	22.326	40.589	0.232	0.027	0.000	0.000
0.15	4.508	2.844	6.096	22.326	40.589	0.461	0.099	0.003	0.000
0.20	6.010	2.844	6.096	22.326	40.589	0.637	0.201	0.010	0.001
0.25	7.513	2.844	6.096	22.326	40.589	0.758	0.312	0.025	0.002
0.30	9.015	2.844	6.096	22.326	40.589	0.838	0.418	0.046	0.005
0.35	10.518	2.844	6.096	22.326	40.589	0.890	0.514	0.075	0.011
0.40	12.020	2.844	6.096	22.326	40.589	0.924	0.596	0.109	0.018
0.45	13.523	2.844	6.096	22.326	40.589	0.947	0.665	0.148	0.028
0.50	15.025	2.844	6.096	22.326	40.589	0.963	0.723	0.189	0.040
0.55	16.528	2.844	6.096	22.326	40.589	0.973	0.771	0.232	0.055
0.60	18.030	2.844	6.096	22.326	40.589	0.981	0.810	0.275	0.072
0.65	19.533	2.844	6.096	22.326	40.589	0.986	0.842	0.319	0.091
0.70	21.035	2.844	6.096	22.326	40.589	0.990	0.868	0.361	0.111
0.75	22.538	2.844	6.096	22.326	40.589	0.992	0.890	0.402	0.133
0.80	24.040	2.844	6.096	22.326	40.589	0.994	0.908	0.441	0.156
0.85	25.543	2.844	6.096	22.326	40.589	0.995	0.922	0.479	0.179
0.90	27.045	2.844	6.096	22.326	40.589	0.997	0.935	0.515	0.204
0.95	28.548	2.844	6.096	22.326	40.589	0.997	0.945	0.548	0.228
1.00	30.050	2.844	6.096	22.326	40.589	0.998	0.953	0.580	0.253

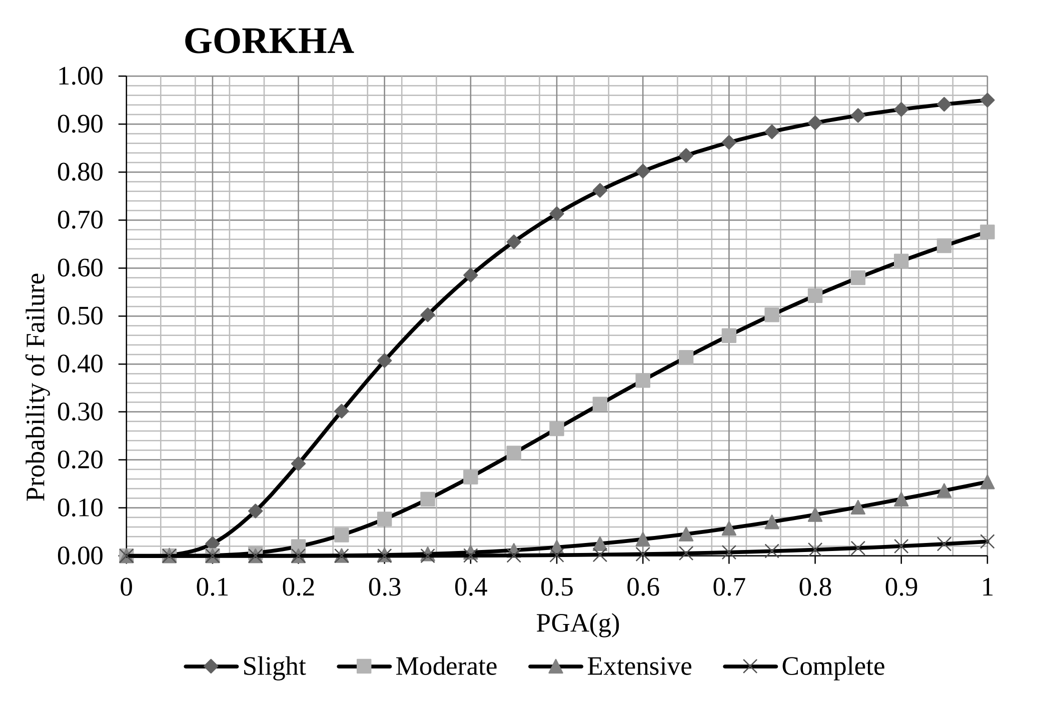

Figure 4-12: Fragility curve for CSEB for various damage state for Gorkha Earthquake

Table 4-22: Calculation of Probability of failure for CSEB (Gorkha Earthquake)

PGA (g)	Top displacement (mm)					Probability of failure at damage state (pf)			
	Demand (mm) Sd	Capacity Displacement mm (Sc)							
	Gorkha	Slight	Moderate	Extensive	Complete	Slight	Moderate	Extensive	Complete
0.00	0.000	0.000	0.000	0.000	0.000	0.000	0.000	0.000	0.000
0.05	0.495	2.844	6.096	22.326	40.589	0.001	0.000	0.000	0.000
0.10	0.990	2.844	6.096	22.326	40.589	0.025	0.001	0.000	0.000
0.15	1.486	2.844	6.096	22.326	40.589	0.094	0.006	0.000	0.000
0.20	1.981	2.844	6.096	22.326	40.589	0.192	0.020	0.000	0.000
0.25	2.476	2.844	6.096	22.326	40.589	0.302	0.044	0.001	0.000
0.30	2.971	2.844	6.096	22.326	40.589	0.407	0.077	0.002	0.000
0.35	3.467	2.844	6.096	22.326	40.589	0.502	0.118	0.004	0.000
0.40	3.962	2.844	6.096	22.326	40.589	0.585	0.164	0.007	0.000
0.45	4.457	2.844	6.096	22.326	40.589	0.655	0.214	0.012	0.001
0.50	4.952	2.844	6.096	22.326	40.589	0.713	0.265	0.018	0.002
0.55	5.447	2.844	6.096	22.326	40.589	0.762	0.316	0.025	0.002
0.60	5.943	2.844	6.096	22.326	40.589	0.802	0.366	0.035	0.004
0.65	6.438	2.844	6.096	22.326	40.589	0.835	0.414	0.045	0.005
0.70	6.933	2.844	6.096	22.326	40.589	0.862	0.459	0.058	0.007
0.75	7.428	2.844	6.096	22.326	40.589	0.884	0.502	0.071	0.010
0.80	7.923	2.844	6.096	22.326	40.589	0.903	0.542	0.086	0.013
0.85	8.419	2.844	6.096	22.326	40.589	0.918	0.580	0.102	0.016
0.90	8.914	2.844	6.096	22.326	40.589	0.931	0.614	0.118	0.020
0.95	9.409	2.844	6.096	22.326	40.589	0.941	0.646	0.136	0.025
1	9.904	2.844	6.096	22.326	40.589	0.950	0.676	0.154	0.030

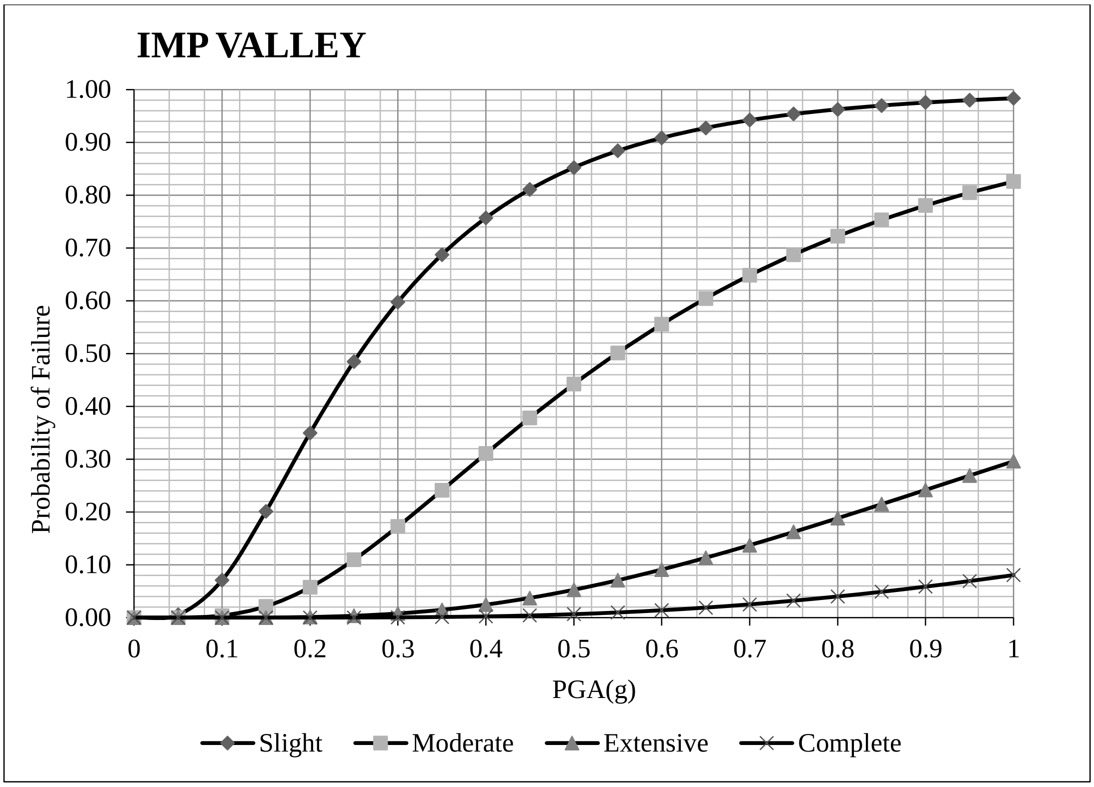

Figure 4-13: Fragility curve for CSEB for various damage state for Imperial Valley Earthquake

Table 4-23: Calculation of Probability of failure for CSEB (Imp Valley Earthquake)

PGA (g)	**Top displacement (mm)**					**Probability of failure at damage state (pf)**			
	Demand (mm) Sd	**Capacity Displacement mm (Sc)**							
	Imp Valley	**Slight**	**Moderate**	**Extensive**	**Complete**	**Slight**	**Moderate**	**Extensive**	**Complete**
0.00	0.000	0.000	0.000	0.000	0.000	0.000	0.000	0.000	0.000
0.05	0.936	2.844	6.096	22.326	40.589	0.005	0.000	0.000	0.000
0.1	1.873	2.844	6.096	22.326	40.589	0.071	0.004	0.000	0.000
0.15	2.810	2.844	6.096	22.326	40.589	0.201	0.021	0.000	0.000
0.2	3.748	2.844	6.096	22.326	40.589	0.349	0.057	0.001	0.000
0.25	4.685	2.844	6.096	22.326	40.589	0.485	0.110	0.003	0.000
0.3	5.622	2.844	6.096	22.326	40.589	0.597	0.173	0.008	0.001
0.35	6.560	2.844	6.096	22.326	40.589	0.687	0.241	0.015	0.001
0.4	7.497	2.844	6.096	22.326	40.589	0.757	0.311	0.025	0.002
0.45	8.434	2.844	6.096	22.326	40.589	0.811	0.378	0.037	0.004
0.5	9.372	2.844	6.096	22.326	40.589	0.852	0.442	0.053	0.006
0.55	10.309	2.844	6.096	22.326	40.589	0.884	0.501	0.071	0.010
0.6	11.246	2.844	6.096	22.326	40.589	0.908	0.555	0.091	0.014
0.65	12.184	2.844	6.096	22.326	40.589	0.927	0.604	0.113	0.019
0.7	13.121	2.844	6.096	22.326	40.589	0.942	0.648	0.137	0.025
0.75	14.058	2.844	6.096	22.326	40.589	0.953	0.687	0.162	0.032
0.8	14.996	2.844	6.096	22.326	40.589	0.962	0.722	0.188	0.040
0.85	15.933	2.844	6.096	22.326	40.589	0.970	0.753	0.215	0.049
0.9	16.871	2.844	6.096	22.326	40.589	0.975	0.780	0.242	0.059
0.95	17.808	2.844	6.096	22.326	40.589	0.980	0.804	0.269	0.069
1	18.745	2.844	6.096	22.326	40.589	0.983	0.826	0.296	0.080

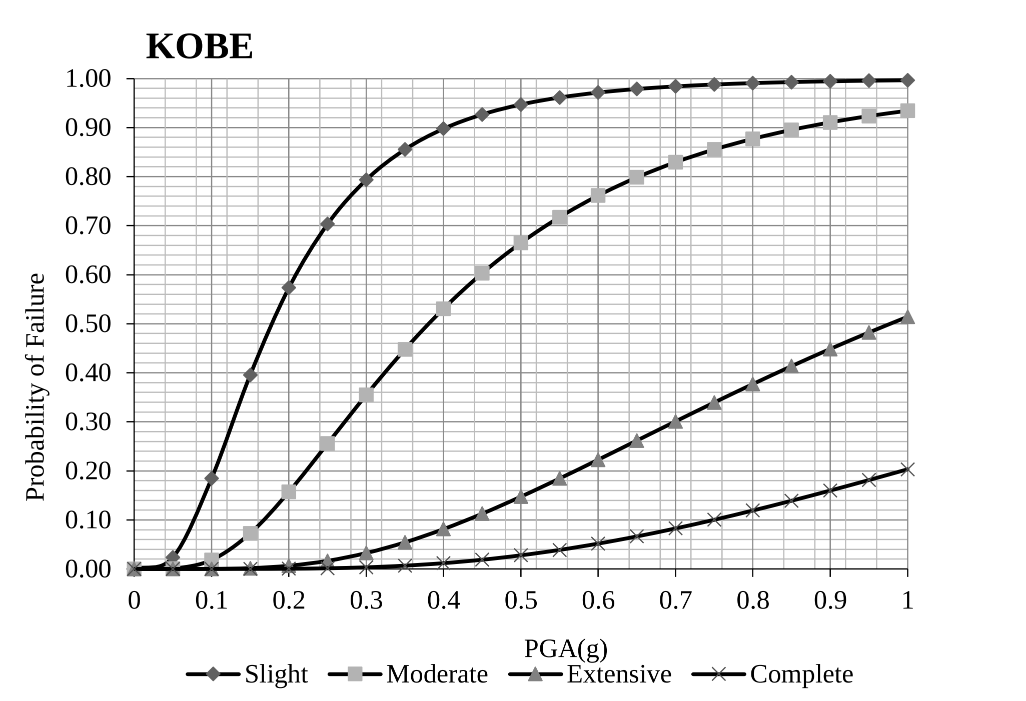

Figure 4-14: Fragility curve for CSEB for various damage state for Kobe Earthquake

Table 4-24: Calculation of Probability of failure for CSEB (Kobe Earthquake)

PGA (g)	Top displacement (mm)					Probability of failure at damage state (pf)			
	Demand (mm) Sd	Capacity Displacement mm (Sc)							
	Kobe	Slight	Moderate	Extensive	Complete	Slight	Moderate	Extensive	Complete
0.00	0.000	0.000	0.000	0.000	0.000	0.000	0.000	0.000	0.000
0.05	1.351	2.844	6.096	22.326	40.589	0.024	0.001	0.000	0.000
0.10	2.702	2.844	6.096	22.326	40.589	0.185	0.018	0.000	0.000
0.15	4.053	2.844	6.096	22.326	40.589	0.396	0.073	0.002	0.000
0.20	5.404	2.844	6.096	22.326	40.589	0.573	0.157	0.007	0.000
0.25	6.756	2.844	6.096	22.326	40.589	0.703	0.256	0.017	0.001
0.30	8.107	2.844	6.096	22.326	40.589	0.793	0.355	0.032	0.003
0.35	9.458	2.844	6.096	22.326	40.589	0.855	0.448	0.054	0.007
0.40	10.809	2.844	6.096	22.326	40.589	0.898	0.471	0.081	0.012
0.45	12.160	2.844	6.096	22.326	40.589	0.927	0.603	0.113	0.019
0.50	13.511	2.844	6.096	22.326	40.589	0.947	0.665	0.147	0.028
0.55	14.862	2.844	6.096	22.326	40.589	0.961	0.717	0.184	0.039
0.60	16.213	2.844	6.096	22.326	40.589	0.971	0.761	0.223	0.052
0.65	17.564	2.844	6.096	22.326	40.589	0.979	0.798	0.262	0.066
0.70	18.915	2.844	6.096	22.326	40.589	0.984	0.829	0.301	0.083
0.75	20.267	2.844	6.096	22.326	40.589	0.988	0.855	0.339	0.100
0.80	21.618	2.844	6.096	22.326	40.589	0.991	0.877	0.377	0.119
0.85	22.969	2.844	6.096	22.326	40.589	0.993	0.895	0.414	0.139
0.90	24.320	2.844	6.096	22.326	40.589	0.994	0.911	0.449	0.160
0.95	25.671	2.844	6.096	22.326	40.589	0.996	0.923	0.482	0.181
1.00	27.022	2.844	6.096	22.326	40.589	0.997	0.934	0.514	0.203

4.5 Cost analysis

4.5.1 General

Nepal has a wide variability in costs due to several factors that are associated with the location of the building (Primarily), the skill of the local builders, availability of material, and the date of construction. Unfortunately, there is little or no data on these aspects (Schildkamp and Araki, 2019). Nepal has a relatively poor transportation system compared to other countries. Materials are sourced from the closest local market if available. Transportation costs are a high proportion of the overall construction in the rural areas of Nepal. Single locations require multiple forms of transport including large trucks, small vehicles (tractors), and finally manual lifting during transportation of material. There are occasionally cases where the vehicles are unable to transport at full capacity due to poor condition of roads which require more trips.

Material is a major component of construction cost and therefore reduction in the cost of material results in a reduction of overall construction cost. In our locality, there are a lot of materials that can be sourced locally for construction purposes. One major way to bring down the cost of material for economically suitable housing is to transfer technology towards the usage of local materials. So, this study focuses on the affordable and safe housing that can be constructed in rural areas of Nepal with different alternatives.

4.5.2 Calculation of quantity of work

Following the detail drawing the quantity of different work to be done is calculated for a different typology of building. The entire building work is subdivided into individual items of works and calculate the different quantities for four types of building. The long wall and short wall methods are adopted to calculate the quantity of different work. In this method length of the longwall is calculated from the center line length of wall and adding half breadth at each end to its center length. The length of short wall measured into in and may be found by deducting half breadth from its center line length at each end. The following table shows that the quantity of the different type of work.

After calculating the different quantities of work, the work is breakdown into different parts. The material and labor required for different work are calculated from Document published by DUDBC- Norms for rate analysis (Civil) works.

Table 4-25: Quantity of work for Different building

S.N	Description of Particulars	Unit	BCEM	SCEM	SMUD	CSEB
1	Site preparation	Sq.m	70.32	76.16	81.20	70.80
2	Earth work in Excavation	Cu.m	17.60	22.27	22.78	17.64
3	Earth filling	Cu.m	10.56	13.36	13.67	10.58
4	Bricksoling	Cu.m	0.99			
5	Stone Soiling	Cu.m		1.67		1.32
6	Wooden plate work at foundation	Cu.m			0.26	
7	PCC 1:1.5:3 (100mm thick)	Cu.m	2.20	2.78		2.20
8	PCC for RCC Bands	Cu.m	5.19	7.18		5.35
9	Wood Work for Timber Band	Cu.m			1.87	
10	Brickwork (1:4)	Cu.m	49.07			
11	Stone Work (1:4)	Cu.m		73.58		
12	Stone Work with mud mortar	Cu.m			98.25	
13	CSEB Work	Cu.m				50.78
14	Wooden work for door and windows	Cu.m	1.15	1.15	1.15	1.15
15	12.5mm Plaster works 1:4	Sq.m	329.18	337.10		329.73
16	Mud Plaster Works	Sq.m			343.70	
17	Painting works	Sq.m	329.18	337.10		329.73
18	Floor work	Sq.m	79.52	88.32	96.00	80.24
19	Roofing works with CGI sheet	Sq.m	57.32	60.90	62.71	57.34

The total number of labor is calculated by breakdown it into superstructure and substructure. The table 4-26 shows the number of labor required for construction purposes for a different building.

Table 4-26: Labors requirement for different typology of building

Building Type	BCEM		SCEM		SMUD		CSEB	
Manpower	Skilled	Unskilled	Skilled	Unskilled	Skilled	Unskilled	Skilled	Unskilled
Sub structure	25.57	74.25	32.34	138.65	32.91	69.47	25.63	74.43
Super structure	260.65	206.43	297.69	428.36	325.61	237.01	263.58	211.37
Total	286.22	280.68	330.03	567.01	358.52	306.47	289.21	285.8

Material required for different work is calculated based on the document available from DUDBC- Norms for rate analysis (Civil) works. Material required for CSEB works is calculated on the basis of the size of a block and cement-sand ratio. The quantity of material required for different work for a building is shown in table 4-27.

Table 4-27: Quantity of material for different building

S.N	Material	Unit	BCEM	SCEM	SMUD	CSEB
1	Brick	No.	27716			
2	Stone	Cu.m		82.69	108.08	
3	CSEB	No.				8531
4	Soil	Cu.m	5.05	5.48	49.84	5.05
5	Cement	M.T	8.86	17.27		7.27
6	C/A	Cu.m	6.34	8.54		6.48
7	F/A	Cu.m	20.12	42.32		15.44
8	Water	Lt	7747.89	9211.09	6877.5	3360.52
9	Re bar	M.T	0.8	0.91		0.8
10	Wire	Kg	7.64	8.71		7.65
11	Husk	Kg			85.93	
12	Cow Dung	Kg			103.11	
13	Timber for Band	Cu.m			1.97	
14	Timber (Door Window frame)	Cu.m	0.58	0.58	0.58	0.58
15	Door window plank	Sq.m	20.9	20.9	20.9	20.9
16	Wood for floor work and staircase	Cu.m	5.23	5.38	5.47	5.23
17	wood for roof	Cu.m	1.75	1.78	1.8	1.75
18	Bamboo	No.	60	62	62	60
19	polythene	Sq.m	48.05	52.22	52.22	48.14
20	Holdfast	No.	49	49	49	49
21	Pin	No.	97	97	97	97
22	handle	No.	28	28	28	28
23	100mm hinge	No.	56	56	56	56
24	locking set	No.	14	14	14	14
25	Keel	kg	10.98	11.12	12.88	10.99
26	CGI sheet 0.24mm-30g	Sq.m	68.8	73.08	75.25	68.8
27	8 mm nut bolt	No.	172	183	188	172
28	J hook	No.	143	152	157	143
29	Bitumen washer	No.	315	335	345	315
30	White cem	Kg	26.24	40.45		26.3
31	Gum	Kg	1.05	1.62		1.05
32	Paint	Kg	65.59	101.13		65.75

CSEB Size 240*240*90
With 10mm thickness of mortar 250*250*100
Number of CSEB required = 160 no
Add 5% wastage CSEB required = 168
Volume of wet mortar = 0.17056 cu.m
Volume of dry mortar (add 30%) = 0.221728
C:S ratio 1:4, Total parts = 5

Cement required = 0.0443 cu.m = 1.28 bags
Sand required = 0.177 cu.m
Water required = 38.58 lit

After finding the labor required for different work and quantity of material. District rate 077/78 of Ramechhap district is used to calculate the total cost of construction for different typology. The cost of CSEB block is calculated by the summation of equipment cost, infrastructure cost, maintenance cost, labor cost and material cost. The cost per CSEB block is calculated as 28.38 without VAT. The following table 4-28 to 4-31 shows that the total cost for a different typologies of building.

Table 4-28: Summary of total cost for SMUD typology

SMUD (Stone with mud mortar)				
Description	Labor (Rs)	Material (Rs)	Total (Rs)	Remark (%)
Plinth (Rs)	92120.03	40635.57	132755.6	10.68
Superstructure (Rs)	444810.15	473949.09	918759.2	73.93
Roof work (Rs)	49010.94	98686.49	147697.4	11.89
Aesthetic (Rs)	41022.74	2428.35	43451.1	3.5
Total (Rs)	626963.86	615699.5	**1242663**	100
Percentage (%)	50.45	49.55	100	

Table 4-29: Summary of total cost for CSEB typology

CSEB (Compressed stabilized earth block with cement sand mortar)				
Description	Labor (Rs)	Material (Rs)	Total (Rs)	Remark (%)
Plinth (Rs)	88735.2	139655.59	228390.8	15.86
Superstructure (Rs)	302241.35	636965.85	939207.2	65.22
Roof work (Rs)	46874.85	94708.37	141583.2	9.83
Aesthetic (Rs)	100166.55	30762.71	130929.3	9.09
Total (Rs)	538017.95	902092.53	**1440110**	100
Percentage (%)	37.36	62.64	100	

Table 4-30: Summary of total cost for BCEM typology

BCEM (Brick with cement sand mortar)				
Description	Labor (Rs)	Material (Rs)	Total (Rs)	Remark (%)
Plinth (Rs)	88524.37	195431.24	283955.6	17.73
Superstructure (Rs)	295240.63	750266.01	1045507	65.27
Roof work (Rs)	46874.85	94708.37	141583.2	8.84
Aesthetic (Rs)	99999.47	30749.07	130748.5	8.16
Total (Rs)	530639.32	1071154.69	**1601794**	100
Percentage (%)	33.13	66.87	100	

Table 4-31: Summary of total cost for SCEM typology

SCEM (Stone with cement sand mortar)				
Description	Labor (Rs)	Material (Rs)	Total (Rs)	Remark (%)
Plinth (Rs)	149377.64	140981.95	290359.6	16.33
Superstructure (Rs)	515288.48	677134.07	1192423	67.06
Roof work (Rs)	48294.41	97353.01	145647.4	8.19
Aesthetic (Rs)	102405.43	47356.31	149761.8	8.42
Total (Rs)	815365.96	962825.34	**1778191**	100
Percentage (%)	45.85	54.15	100	

4.5.3 Use of local building material in different typology

In rural areas of Nepal, there are various types of building materials that can be sourced locally for construction purpose for different typology. Material is a major component of construction cost in building and a reduction in the cost of material can also result to a reduction in overall construction cost. One major way to bring down the cost of building materials is to shift toward the usage of local materials.

In most of the rural areas of Nepal, different building materials like stone, soil, wood, bamboo, and aggregate can be sourced locally whereas brick, cement, rebar, CGI sheet, paint, fixtures for door and roof have to buy from the market. The following table 4-32 and 4-33 shows the percentage of use of different materials in terms of cost for different typologies. For manufacturing of CSEB block, 68.65% of the cost can be sourced locally and 31.35 % of CSEB cost must be purchased from the market.

Table 4-32: Quantity of material (%) for BCEM and SCEM building typology

BCEM				SCEM		
S.N	**Material**	**Cost (Rs)**	**Material (%)**	**Material**	**Cost (Rs)**	**Material (%)**
1	Brick	407142	38.01	Stone	98115.8	10.19
2	Cement	135227	12.62	Cement	263469	27.36
3	Aggregate	57932.2	5.41	Aggregate	111589	11.59
4	Rebar and wire	69330.1	6.47	Rebar and wire	79068.6	8.21
5	Wood	330833	30.89	Wood	334499	34.74
6	Bamboo	15255	1.42	Bamboo	15750.8	1.64
7	Polythene	1357.51	0.13	Polythene	1475.07	0.15
8	Soil and Water	5410.15	0.51	Soil and Water	6102.48	0.63
9	CGI sheet	22015.1	2.06	CGI sheet	23387.2	2.43
10	Fixtures for door, window and roof	20880.2	1.95	Fixtures for door, window and roof	20467.8	2.13
11	Finishing material	5772.12	0.54	Finishing material	8899.88	0.92
12	Total	1071155	100	Total	962825	100

Table 4-33: Quantity of material (%) for CSEB and SMUD building typology

CSEB				**SMUD**		
S.N	**Material**	**Cost (Rs)**	**material (%)**			
1	CSEB	273568.4	30.33	**Material**	**Cost (Rs)**	**material (%)**
2	Cement	110951.9	12.3	Stone	128230.99	20.83
3	Aggregate	47923.25	5.31	Soil	29845.989	4.85
4	Rebar and wire	69433.37	7.7	Wood	388414.73	63.09
5	Wood	330833.2	36.67	Bamboo	18550.928	3.01
6	Bamboo	15163.47	1.68	Polythene	1475.0738	0.24
7	Polythene	1359.91	0.15	Water	1942.8938	0.32
8	Soil and Water	4176.41	0.46	CGI sheet	24081.837	3.91
9	CGI sheet	22015.11	2.44	Finishing material	2428.3522	0.39
10	Fixtures for door, window and roof	20881.73	2.31	Fixtures for door, window and roof	20728.707	3.37
11	Finishing material	5785.77	0.64	Total	615699.5	100
12	Total	902092.5	100			

4.6 Discussion

Storey displacement (mm) and storey drift (%) of buildings at different PGA (g) of three different earthquake scenarios are determined from linear dynamics analysis of the buildings. The storey displacement (mm) table 4-1 to 4-12 shows displacement goes on increasing with the storey height at particular PGA (g) and, maximum drift ratio occurs at the first floor. Also, it is observed that the storey drift for all stories is found to be within the permissible limits. The displacement and Base shear of different building vary linearly with an increase in PGA (g). This is due to linear time history has shown all parameters vary linearly along with Sa/g.

Lateral displacement and storey drifts are considerably reduced while the contribution of brick wall with cement mortar (BCEM) is taken into account. Characteristics of masonry walls influence the overall behavior of structures when subjected to lateral force.

For the same PGA value of different earthquake data is found to be different for same building which is due to parameters associated with time history function like frequency content and duration.

Analytical fragility curves are drawn in Figure for different types of buildings and different earthquake respectively. The fragility curves for various levels of damage state for each type of building are shown in Figure. According to the seismic hazard analysis map of Nepal, it is shown that PGA for 10% probability of exceedance in 50 years (return period 475 years) is expected to be 0.4g (BCDP 1994). Therefore, the probability of failure is observed at the PGA value of 0.4g for each type of building.

Figure 4-15 shows that the probability of failure of different building at 0.4g of Gorkha earthquake. Building BCEM has a 49.68% chance of experiencing Slight damage, 11.53% chance of experiencing moderate damage, no chance of experiencing extensive damage and complete damage. Analyzing these probabilities, the building is expected to have no/slight damage state as the probability of failure below 50% in slight damage condition.

Similarly, other types of buildings are also analyzed. Building SCEM, SMUD and CSEB are also expected to have slight to moderate damage since their probabilities of failure (52.37%, 61.47% and 58.48%) respectively) at PGA of 0.4g of Gorkha earthquake.

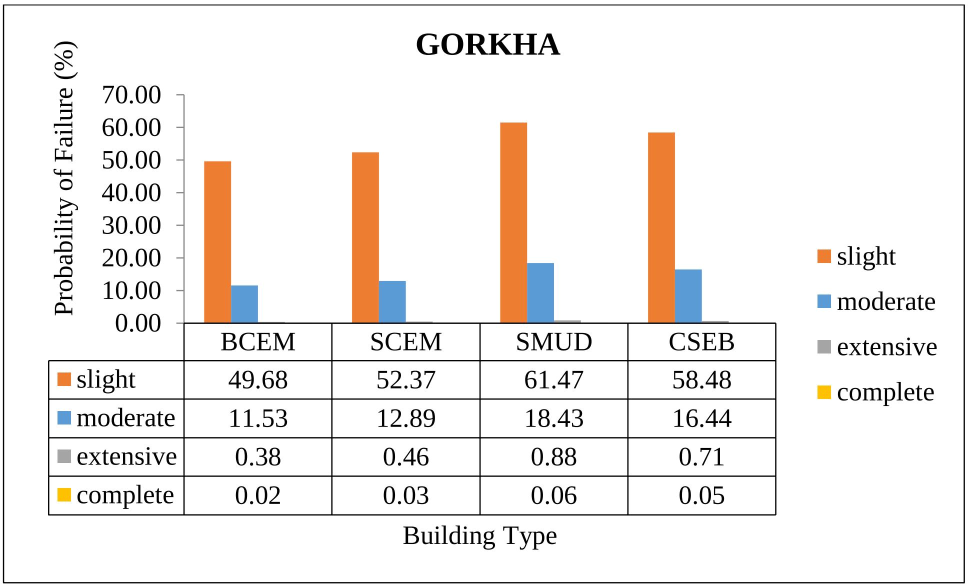

	BCEM	SCEM	SMUD	CSEB
slight	49.68	52.37	61.47	58.48
moderate	11.53	12.89	18.43	16.44
extensive	0.38	0.46	0.88	0.71
complete	0.02	0.03	0.06	0.05

Figure 4-15: Probability of failure of building for PGA=0.4g for Gorkha earthquake

Figure 4-16 shows that the probability of failure of different building at 0.4g of Imp Valley earthquake. Building BCEM has 59.60% chance of experiencing Slight damage, 17.17% chance of experiencing moderate damage, no chance of experiencing extensive damage and complete damage. Analyzing these probabilities, the building is expected to have moderate damage state as the probability of failure below 50% in moderate damage condition.

Similarly, other types of buildings are also analyzed. Building SCEM, SMUD and CSEB are also expected to have slight to moderate damage since their probabilities of failure (20.22%, 48.01% and 31.05%) respectively) at PGA of 0.4g of Imp Valley earthquake.

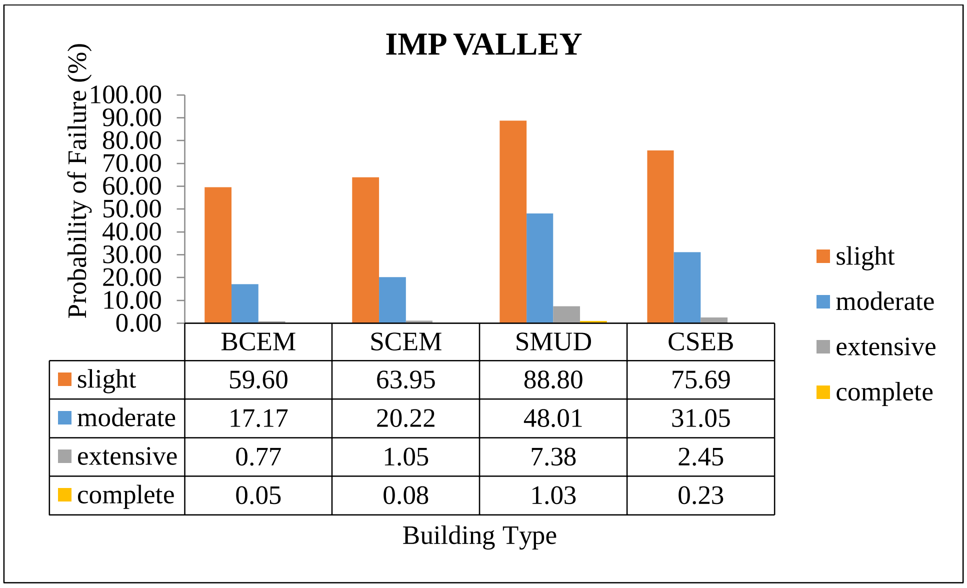

	BCEM	SCEM	SMUD	CSEB
slight	59.60	63.95	88.80	75.69
moderate	17.17	20.22	48.01	31.05
extensive	0.77	1.05	7.38	2.45
complete	0.05	0.08	1.03	0.23

Figure 4-16: Probability of failure of building for PGA=0.4g for Imp Valley earthquake

Figure 4-17 shows that the probability of failure of different building at 0.4g of Kobe earthquake. Building BCEM has a 73.65% chance of experiencing Slight damage, 28.84% chance of experiencing moderate damage, no chance of experiencing extensive damage and complete damage. Analyzing these probabilities, the building is expected to have slight/moderate damage state as the probability of failure below 50% in moderate damage condition.

Similarly, other types of buildings are also analyzed. Building SCEM, SMUD and CSEB are also expected to have moderate damage since their probabilities of failure (29.09%, 59.61% and 47.08% at moderate damage condition) respectively) at PGA of 0.4g of Kobe earthquake.

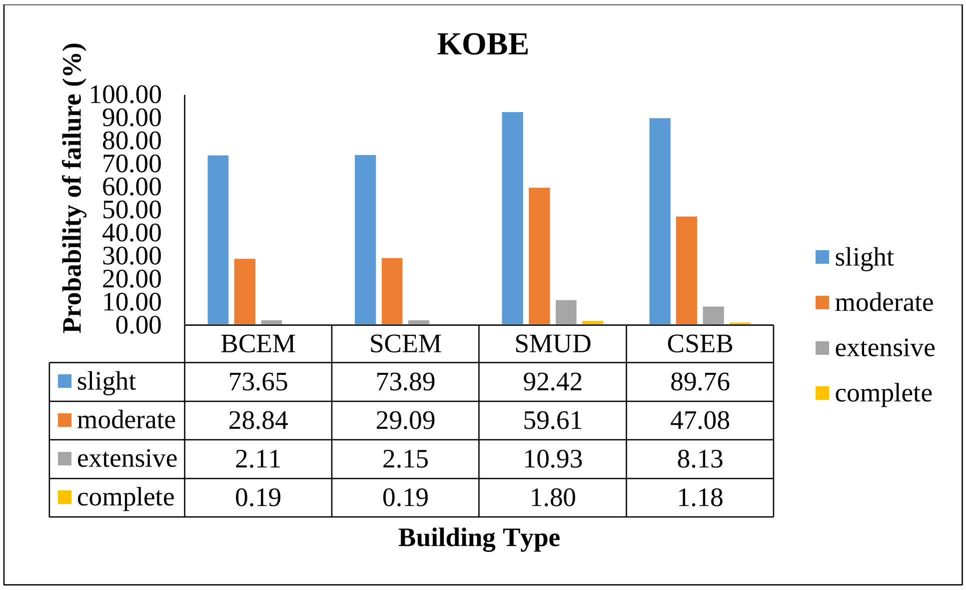

Figure 4-17: Probability of failure of building for PGA=0.4g for Kobe earthquake

The probability of failure of buildings in the same PGA of a different earthquake is varied i.e., high in Kobe than Imp Valley and Gorkha. This may be due to the variations in modal frequencies and predominant frequencies of ground motions. The probability of failure of a different building is small percent in the analysis of houses applying the Gorkha Earthquake than the other two earthquake (Imp Valley and Kobe) histories. Hence the performance of a building by following NBC code and standard can standby against the different types of earthquake-like Gorkha Earthquake with less damage and are suitable in terms of seismic performance.

The total number of labor is calculated by breakdown it into superstructure and substructure. After that total number of labor required for different typology is calculated by adding labor required for substructure and superstructure. The figure 4-18 shows the number of laborers required for construction purposes for the different typologies of buildings. The total number of labor required to construct BCEM typology is 566.9. Similarly, the labor required for SCEM, SMUD, and CSEB is 897.04, 664.99, and 575.01. The variation in the total number of labor is due to variation in material type and construction technology used in different typologies.

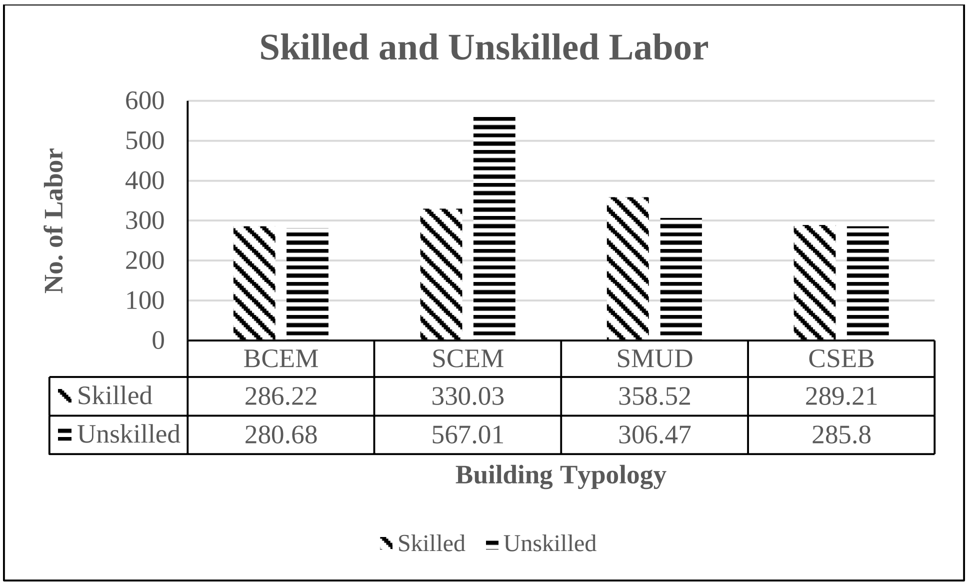

Figure 4-18: Labor required for different typology of building

The total cost of building is calculated by adding material cost and labor cost. The figure 4-19 shows the material cost and labor cost for different typologies. From the graph, it has shown that the labor cost of SCEM building is highest among four typologies i.e., 8, 15,365.96 and the material cost of BCEM building is highest among four typologies i.e., 10, 71,154.69. The total cost of SMUD building is lowest among four typologies i.e., 12, 42,663.36 which is 13.71% lower than CSEB building, 22.42% lower than BCEM building, and 30.12% lower than SCEM building.

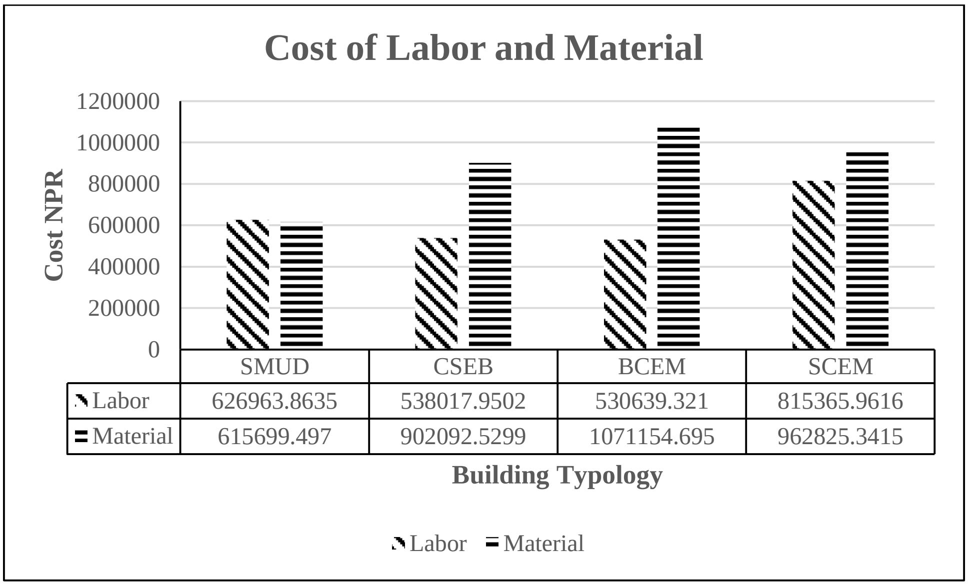

Figure 4-19: Cost of different typology (Labor and material)

The figure 4-20 shows that the use of local and commercial materials to construct a different typology of building. In most of the rural areas of Nepal, different building materials like stone, soil, wood, bamboo, and aggregate can be sourced locally whereas brick, cement, rebar, paint, CGI sheet, fixtures for door and roof have to buy from the market. The graph shows that 92.09% of the material can be sourced locally for SMUD building typology. Similarly, 64.95%, 58.79%, and 38.22% of the material can be sourced locally for CSEB, SCEM, and BCEM buildings respectively.

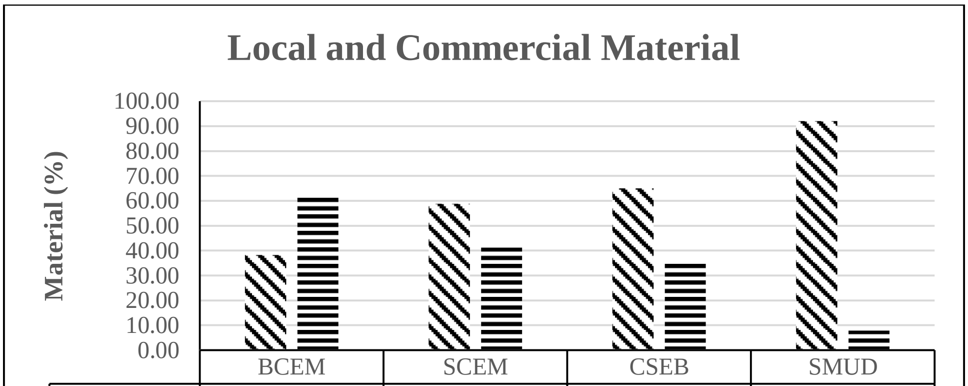

	BCEM	SCEM	CSEB	SMUD
Local	38.22	58.79	64.95	92.09
Commercial	61.78	41.21	35.05	7.91

Figure 4-20: Use of local and commercial material for different typology

4.6.1 Suitability of Building

For the suitability of building weighted average method is used as a statistical method. Seismic performance percentage is taken in terms of probability of failure at Kobe earthquake because of the effect of Kobe earthquake is highest among three earthquake for all typology. Cost of building is taken as percentage by changing cost into standard percentage. Here, the percentage of cost of SCEM typology is taken as 100% because of the cost of SCEM typology is highest for Rammechhap district. Use of commercial material in building is taken as percentage.

Weighted average is a calculation that takes into account the varying degrees of importance of the numbers in a data set. Weight of every parameter is assumed to be equal for this research purpose. By using average weightage method average percentage of each typology is calculated.

Calculation

For BCEM typology

Probability of failure = 28.84%

Percentage of cost = $\frac{1601794}{1778191}$ = 90.08%

Material = 61.78%

Assigning equal weight of each item i.e. $\frac{1}{3}$ and multiplying by weight of each item

Probability of failure = 28.84*1/3 = 9.61%

Percentage of cost = 90.08*1/3= 30.03%

Material = 61.78*1/3 = 20.59%

Total weight of BCEM typology = 9.61+30.03+20.59 = 60.23%

Table 4-34: Percentage of each item

Typology	Failure (%)	Cost (%)	Commercial Material (%)
BCEM	28.84	90.08	61.78
SCEM	29.09	100	41.21
SMUD	59.61	69.88	7.91
CSEB	47.08	80.99	35.05

Table 4-35: Weightage percentage of each typology

Typology	Failure (%)	Cost (%)	Commercial Material (%)	Total (%)
BCEM	9.61	30.03	20.59	60.23
SCEM	9.70	33.33	13.74	56.77
SMUD	19.87	23.29	2.64	45.80
CSEB	15.69	27.00	11.68	54.37

From above table the weightage percentage of SMUD typology is lowest and BCEM typology is highest. So, SMUD typology is suitable among four typology in terms of seismic performance, cost and use of local material.

5 CONCLUSION

5.1 General

Four buildings of different typologies and the same floor type and plan are taken for the analysis. A masonry wall is modeled as a bi-linear thin shell element and a timber floor element is modeled as a three-dimensional linear beam element hinged at wall support. Horizontal bands are modeled as a frame element. SAP 2000 V22 is used for the modeling. The seismic input is taken as three earthquakes (Gorkha, Imperial Valley, Kobe) ground motions histories with varying levels of peak ground acceleration. The displacement and base shear are shown in the table 4-1 to 4-12. The fragility curve for a different building is shown in the figure 4-1 to 4-12 above. A fragility curve can be used to find the probability of failure in four damage states (slight, moderate, extensive, complete) at different PGA for a different earthquake. The quantity of material and labor required is calculated by breakdown total work into specific work. The construction cost of each typology is calculated by using the district rate (2077/78) of the Ramechhap district.

5.2 Conclusion

The following major conclusions are drawn from the current research.

1. Lateral displacement and storey drifts are considerably less in BCEM typology than that of SCEM, CSEB, and SMUD typology. Characteristics of masonry walls influence the overall behaviour of structures when subjected to lateral force.
2. The base shear of SMUD typology is more than that of BCEM, SCEM and CSEB typology. It is due to the heavyweight of wall and the characteristics of the material.
3. For the same value of PGA and same type of building, the displacement value of the Kobe earthquake is highest and the Gorkha earthquake is lowest, which is due to parameters associated with time history function like frequency content and duration.
4. For the same earthquake, the probability of failure of SMUD typology is 12.53% to 30.77% more than that of other typology. This is due to the variation in material properties and thickness of the wall of each typology.

5. For the same value of PGA, the probability of failure due to seismic input Kobe is highest and that of Gorkha is lowest.
6. Considering the same plan and elevation, the total number of labor required to construct SCEM typology is the highest among the four typologies.
7. For rural area SMUD typology is most suitable in terms of seismic performance, cost and use of local material.

5.3 Recommendations for further study

Different assumptions and limitations have been adopted for simplicity in modelling and analysis. The following recommendations are made for further study:

1. Experimental testing of stone, brick and CSEB panel for obtaining the material properties.
2. Though, the masonry is heterogeneous the masonry wall is assumed to be homogenous element, the study can be extended with detailed micro-modelling.
3. Non-linear time history analysis for response analysis can be done.
4. Development of suitable retrofitting technique for masonry structure.

REFERENCES

Gautam, D., Rodrigues, H., Bhetwal, K. K., Neupane, P., & Sanada, Y. (2016). Common structural and construction deficiencies of Nepalese buildings. Innovative Infrastructure Solutions, 1(1), 1-18.

Dixit, A. M., Parajuli, Y. K., & Guragain, R. (2004, August). Indigenous skills and practices of earthquake resistant construction in Nepal. In 13th World Conference on Earthquake Engineering (pp. 1-6).

Ali, Q., Khan, A. N., Ashraf, M., Ahmed, A., Alam, B., Ahmad, N, & Umar, M. (2013). Seismic performance of stone masonry buildings used in the Himalayan Belt. Earthquake Spectra, 29(4), 1159-1181.

Karaşin, İ. B., Bakir, D., Ülker, M., & Emre, A. (2017). The Structural Damages After Nepal Earthquakes. IOSR Journal of Engineering (pp. 45-54)

Gautam, D. (2018). Observational fragility functions for residential stone masonry buildings in Nepal. Bulletin of Earthquake Engineering, 16(10), 4661-4673.

Gautam, D., & Chaulagain, H. (2016). Structural performance and associated lessons to be learned from world earthquakes in Nepal after 25 April 2015 (MW 7.8) Gorkha earthquake. Engineering Failure Analysis, 68, 222-243.

HRRP (2018). *Housing Typologies: Earthquake Affected Districts*. Housing Recovery and Reconstruction Platform.

CBS (2012). National Population and Housing Census 2011 (National Report). Central Bureau of Statistics, Kathmandu, Nepal

DUDBC Vol I, Vol II (2015). Design Catalogue For Reconstruction Of Earthquake Resistant Houses. Department of Urban Development and Building Construction, Babarmahal, Kathmandu

Phaiju, S., & Pradhan, P. M. (2018). Experimental work for mechanical properties of brick and masonry panel. *Journal of Science and Engineering*, *5*, 51-57.

Magenes, G., Penna, A., Galasco, A., & Rota, M. (2010, July). Experimental characterisation of stone masonry mechanical properties. In *Proceedings of the 8th International Masonry Conference* (pp. 247-256).

Meimaroglou, N., & Mouzakis, H. (2018). Mechanical properties of three-leaf masonry walls constructed with natural stones and mud mortar. *Engineering Structures*, *172*, 869-876.

Steinert, A., & Mellegård, H. (2016). *Compressed Stabilised Earth Blocks in Nepa l-A study of the rehabilitation of rural villages in Nepal after the Gorkha earthquake* (Master's thesis).

Shrestha, H. D., (2012). Standard norms and Specification for CSEB Blocks. Government of Nepal, Ministry of education, Kathmandu Nepal.

Tomazevic, M. (1999). *Earthquake-resistant design of masonry buildings* (Vol. 1). World Scientific.

Salmanpour, A. H., Mojsilovic, N., & Schwartz, J. (2013). Deformation capacity of unreinforced masonry walls subjected to in-plane loading: a state-of-the-art review. *International Journal of Advanced Structural Engineering*, *5*(1), 1-12.

Fonseca, F. S., Mohamad, G., Lourenço, P. B., Roman, H. R., & Vermeltfoort, A. T. (2015, May). Deformation and failure mode of masonry. In *12th North American Masonry Conference, Denver, Colorado*.

Magenes, G., & Calvi, G. M. (1997). In-plane seismic response of brick masonry walls. *Earthquake engineering & structural dynamics*, *26*(11), 1091-1112.

Zhuge, Y., Thambiratnam, D., & Corderoy, J. (1998). Nonlinear dynamic analysis of unreinforced masonry. *Journal of structural engineering*, *124*(3), 270-277.

Abrams, D. P. (2001). Performance-based engineering concepts for unreinforced masonry building structures. *Progress in Structural Engineering and Materials*, *3*(1), 48-56.

Lourenço, P. B., Zucchini, A., Milani, G., & Tralli, A. (2006). Homogenisation approaches for structural analysis of masonry buildings.

DeJong, M. J., Belletti, B., Hendriks, M. A., & Rots, J. G. (2009). Shell elements for sequentially linear analysis: lateral failure of masonry structures. *Engineering Structures*, *31*(7), 1382-1392.

Tena-Colunga, A., & Abrams, D. P. (1996). Seismic behavior of structures with flexible diaphragms. *Journal of Structural Engineering*, *122*(4), 439-445.

Cardoso, R., Lopes, M., & Bento, R. (2005). Seismic evaluation of old masonry buildings. Part I: Method description and application to a case-study. *Engineering structures*, *27*(14), 2024-2035.

Maharjan, A., & Parajuli, H. R. (2020). Seismic Performance Evaluation of Stone Masonry Houses Constructed with Reinforced Concrete Bands. *Nepal Journal of Science and Technology*, *19*(1), 204-214.

Sucuoğlu, H., & Erberik, A. (1997). Performance evaluation of a three-storey unreinforced masonry building during the 1992 Erzincan earthquake. *Earthquake engineering & structural dynamics*, *26*(3), 319-336.

Benedetti, D., & Castellani, A. (1980). Dynamic versus static behaviour of a masonry structure undser lateral loads. *Engineering Structures*, *2*(3), 163-170.

Magenes, G., Penna, A., Senaldi, I. E., Rota, M., & Galasco, A. (2014). Shaking table test of a strengthened full-scale stone masonry building with flexible diaphragms. *International Journal of Architectural Heritage*, *8*(3), 349-375.

Bakhshi, A., & Karimi, K. (2008). Performance evaluation of masonry buildings using a probabilistic approach.

Colangelo, F. (2008). On the computation of seismic fragility curves. In *14th World Conference On earthquake engineering*.

Rota, M., Penna, A., & Magenes, G. (2008). A procedure for deriving analytical fragility curves for masonry buildings. In *14th world conference on earthquake engineering. Beijing, China*.

Tremayne, B., & Kelly, T. E. (2005). Time history analysis as a method of implementing performance based design. *Holmes Consulting Group, Auckland, New Zealand*.

NBC-105, 2020. Nepal National Building Code for Seismic Design of Buildings in Nepal, Ministry of Urban Development, Kathmandu, Nepal.

NBC-109, 1994. Nepal National Building Code for Masonry: Unreinforced, Ministry of Physical Planning and Works, Department of Urban Development and Building Construction, Kathmandu, Nepal.

NBC-202, 2015. Nepal National Building Code for Guidelines on: Load Bearing Masonry, Ministry of Urban Development, Department of Urban Development and Building Construction, Kathmandu, Nepal.

NBC-203, 2015. Nepal National Building Code for Guidelines for Earthquake Resistant Building Construction: Low Strength Masonry, Ministry of Urban Development, Department of Urban Development and Building Construction, Kathmandu, Nepal

Gambarotta, L., & Lagomarsino, S. (1996, September). On dynamic response of masonry panels. In *Proceedings of National Conference on Masonry Mechanics between Theory and Practice, Messina, Italy*.

Senaldi, I., Magenes, G., & Penna, A. (2010). Numerical investigations on the seismic response of masonry building aggregates. In *Advanced Materials Research* (Vol. 133, pp. 715-720). Trans Tech Publications Ltd.

Beyer, K., & Bommer, J. J. (2007). Selection and scaling of real accelerograms for bi-directional loading: a review of current practice and code provisions. *Journal of earthquake engineering*, *11*(S1), 13-45.

Clough, R. W., & Penzien, J. (2003). Dynamics of structures. Berkeley. *CA: Computers and Structures*.

HAZUS 4.2 SP3 . (2020).*Hazus Earthquake Model Technical Manual*. Department of Homeland Security Emergency Preparedness and Response Directorate, FEM Mitigation Division, Washington, D.C.

Schildkamp, M., & Araki, Y. (2019). Cost Analysis of Mountain Schools in Nepal: Comparison of Earthquake Resistant Features in Rubble Stone Masonry vs. Concrete Block Masonry. Frontiers in Built Environment, 5, 55.